LIMNOLOGY
and
OCEANOGRAPHY: METHODS

Limnol. Oceanogr.: Methods 10, 2012, 681–710

Getting good particles: Accurate sampling of particles by large volume in-situ filtration

James K.B. Bishop[1,2], Phoebe J. Lam[3], and Todd J. Wood[2]*
[1]Department of Earth and Planetary Science, University of California, Berkeley, Berkeley, CA 94720
[2]Earth Sciences Division, Lawrence Berkeley National Laboratory, Berkeley, CA 94720
[3]Department of Marine Chemistry and Geochemistry, Woods Hole Oceanographic Institution, Woods Hole, MA 02540

Abstract

We deployed the Multiple Unit Large Volume in-situ Filtration System (MULVFS) to simultaneously sample 12 depths between 10 and 900 m during the US GEOTRACES Atlantic and Pacific intercalibration experiments. Sampling was designed to simultaneously compare large (>51 µm) and small (micron or sub-micron to 51 µm) size particulates collected by four classes of 142 mm filter holders against those collected using the main MULVFS filter holder. We evaluated Whatman "QMA," Pall "Supor" (0.8, 0.45, 0.2 µm), and Millipore "MF" (0.45 µm) filters. Paired QMA filters had best particle loading and uniformity and sample particles to 0.8 µm. Paired 0.8 µm Supor filters sample particles to 0.45 µm and provide the best compromise in terms of sample loading and evenness of particle distribution for elements that require total sample digestion. We also found, under the most benign oceanographic conditions, that many 142 mm single and double baffle filter holders lost of up to 90% of the large particle size fraction, especially in the upper 150 m. We designed and validated a new 142 mm filter holder that solves this problem. We further studied the effect of filtration flow rate on large particle size distribution and chemistry; samples from 500-800 m in the oligotrophic Pacific showed a 50% decrease of > 51 µm Mn, Ba, and Ca (but no effect on P) over a flow velocity range of 0.1 to 1.6 cm s^{-1}. We recommend sampling below 1 cm s^{-1}. The methodology of bottle and in-situ filtration is also discussed.

Adequate sampling of marine particles in large and small size fractions is a key requirement for the international GEOTRACES program, whose aim is to understand the processes that govern the large-scale distributions of key trace elements and isotopes in the ocean (GEOTRACES 2006). Suspended (or small) marine particles are typically sampled through on-deck filtration of water collected from GO-flo or Niskin bottles for small (<30 L) volumes, while in-situ filtration using pumps for larger volumes (hundreds to thousands of liters) captures both suspended and sinking fractions (Bishop and Edmond 1976). The goal of our participation in the GEOTRACES intercalibration expeditions was to eliminate method and PI-dependent differences in particle sampling for GEOTRACES. Here, we focus on resolving sampling issues for particles collected by large volume in-situ filtration. Further comparisons between particles collected by on-deck filtration from bottles and in-situ pump filtration are addressed in a separate article (Planquette and Sherrell 2012). Analytical intercomparisons will be addressed at a later date.

Large volume in-situ filtration enables the collection of size-fractionated marine particles from hundreds to more than ten thousand liter volumes of seawater. In-situ filtration systems in current use include ship-powered systems such as the Multiple Unit Large Volume in-situ Filtration System (MULVFS) (Bishop et al. 1985; Bishop and Wood 2008) and commercially available battery-operated systems such as the McLane Large Volume Water Transfer System (WTS-LV, or "McLane pumps") and the Challenger Oceanic Stand Alone Pumps (SAPs). Before commercial battery powered systems, many variants of pumps were built (Krishnaswami et al. 1976; Bacon and Anderson 1982; Simpson et al. 1987; Wakeham and Canuel 1988; Sachs et al. 1989; Sherrell 1991).

*Corresponding author: E-mail: jkbishop@berkeley.edu

Acknowledgments

We thank Bradley Moran, Ken Buesseler, and Rob Sherrell for letting us borrow their filter holders for testing on the first GEOTRACES intercalibration cruise; Ken Buesseler and Kanchan Maiti for access to the McLane pump rosette and for on-board ^{234}Th counts of prefilter particles; Mark St. Pierre for machining mini-MULVFS holders; Rob Sherrell for productive discussions at sea and for major help with filter tests. We thank Greg Cutter (chief scientist), and the captain and crew of R/V *Knorr* for their assistance. Alejandro Morales, Marty Fleisher, Henrieta Dulaiova, and Jess Fitzsimmons helped with MULVFS deployments. We thank reviewers of this manuscript for their comments and suggestions. This work was supported by NSF grants OCE-0826514 and 0826335 to J.K.B.B. and OCE-0824491 and OCE-0824490 to P.J.L.

DOI 10.4319/lom.2012.10.681

Bottle versus pump discrepancies for particulate organic carbon (POC) and suspended particulate mass (SPM) concentration have been reported in the past (e.g., Bishop and Edmond 1976; Bishop 1999; Altabet et al. 1992; Gardner et al. 2003; Liu et al. 2005, 2009). The three most recent papers have called into question in-situ filtration sampling. Gardner et al. (2003) compared in situ filtration samples collected using Challenger Oceanic pumps and McLane pumps with bottle filtration results collected during the U.S. JGOFS program in the Ross Sea and Antarctic Polar Front Zone. Some pump POC results were 200 times lower than filtered bottle samples, especially those from shallow waters. Liu et al. (2005) sampled Mediterranean waters and reported differences in samples collected using Challenger Oceanic pumps and bottle samples and again found pump samples yielding lower concentrations of large particles in shallow waters. Bishop and Wood (2008) analyzed size fractionated samples collected using MULVFS pumps from the surface to 1000 m from the biologically productive waters of the Oyashio and from highly oligotrophic waters near the site of the Hawaii Ocean Time Series Station (HOT). They addressed the Gardner et al. (2003) and Liu et al. (2005) findings and did not find evidence of bias in MULVFS samples but listed multiple contributors to such biases, including particle washout from filter holders after sampling. A follow-up study by Liu et al. (2009) confirmed that particle washout from in-situ pumps might be a problem.

All studies to date have had difficulty separating causes of sample variability due to natural temporal/spatial patchiness of particle fields from those due to method dependent variables such as filter pore size, filter holder design, water filtration flow velocity, filtration pressure differential, post filtration back flow, filter disturbance by expanding gases cavitated from seawater during pump operation as pumps are returned to the surface, and post collection sample preservation (Bishop and Wood 2008). In this study, we eliminate the differences in place and time of sampling using the multi-flow capability of the MULVFS (Bishop et al. 1985; Bishop and Wood 2008) as the main testing platform for our experiments. We also used a novel in-situ pump rosette (Maiti et al. in press), which permitted simultaneous collection of samples at a single depth using eight McLane pumps.

We evaluate a number of different micron and sub-micron filter types suitable for collecting particles for trace element and isotope analysis. We assess the performance of filter holders and filter types using photographic and chemical analyses of collected particles. We specifically address the hypothesis that some in-situ pump filter holder designs suffer from particle washout, and especially so in the upper 100-200 m. We examine four classes of 142 mm filter holder designs in present use for the purpose of collecting size-fractionated particles for trace element and isotope analysis, including variations within each class. Holders were both homemade and commercial. We present a new 142 mm filter holder design that solves the particle loss problem. Finally, we investigate the effects of sampling velocity on particle collection efficiency.

Materials and procedures

Hydrography and particle optics

CTDs deployed during rosette water sampling and in-situ filtration system profiling were augmented with optical sensors for particles. Profiles of particle beam attenuation coefficient (c_p – units of m^{-1}) at 660 nm and turbidity (units of mFTU) at 810 nm were obtained using a 25 cm path length C-Star transmissometer (WET Labs) and a turbidity sensor (gain 100, Seapoint Sensors), interfaced to the Sea Bird 911 CTD on the GEOTRACES trace metal (TM) rosette. The transmissometer was strapped horizontally to a polypropylene plate attached to the rosette frame. The turbidity sensor was oriented to view open water. Similar data were obtained using a vertically mounted WET Labs. C-Rover transmissometer and Seapoint turbidity sensor interfaced to a Sea Bird 19plus logging CTD deployed at the end of the wire during MULVFS and McLane pump profiles. The C-Rover c_p data were scaled down by 20% to compensate for differences between receiver acceptance angle of the C-Rover and C-Star instruments (see Bishop and Wood 2008). The C-Rover data were further corrected to compensate for a depth (pressure) dependent transmission decrease of 0.44% per kilometer.

Optics cleaning, sensitivity drift tracking, and data processing followed the protocols of Bishop and Wood (2008). Predeployment and postdeployment air calibrations showed that the C-Star transmissometer drifted less than 0.1% in transmission during the 24 and 35 h operation during the two cruises, respectively, and linear adjustments to sensitivity were made proportional to time elapsed. No cast-to-cast offsets were needed. After IC2, it was discovered that an electrical ground fault induced corrosion of the C-Star transmissometer and comparisons with C-Rover transmissometer data indicate that resulting beam attenuation coefficient data were 0.005 m^{-1} low; all profiles have been adjusted upwards accordingly.

Sampling platform

MULVFS consists of 12 ship-electricity (480 VAC, 3 phase) powered pump units deployed simultaneously in an array to kilometer depths using a unified 1000 m long plastic jacketed electromechanical cable. Each pump unit can collect samples of particulate and dissolved species using three flow paths, allowing the simultaneous collection of particles from three kinds of filter holders: the main 293 mm holder, the auxiliary 142 mm holder, and multiple side-arm 47 mm holders (Fig. 1A). Size-fractionated particles were collected on the main and auxiliary flow paths using a 51 µm polyester prefilter and a variety of micron and submicron filter types. The 47 mm side-arm filter holders, with and without prefilter were loaded with 0.45 µm Supor filters. Check and gas release (de bubbler) valves (Fig. 1) protect filter samples from the effects of back flow, contamination, and disruption due to trapped air on deployment and degassed air expansion on recovery. The latter is a problem in shallow samples.

Blank filter suites were loaded onto the deepest pump on each cast, which was electrically disconnected. These "dipped

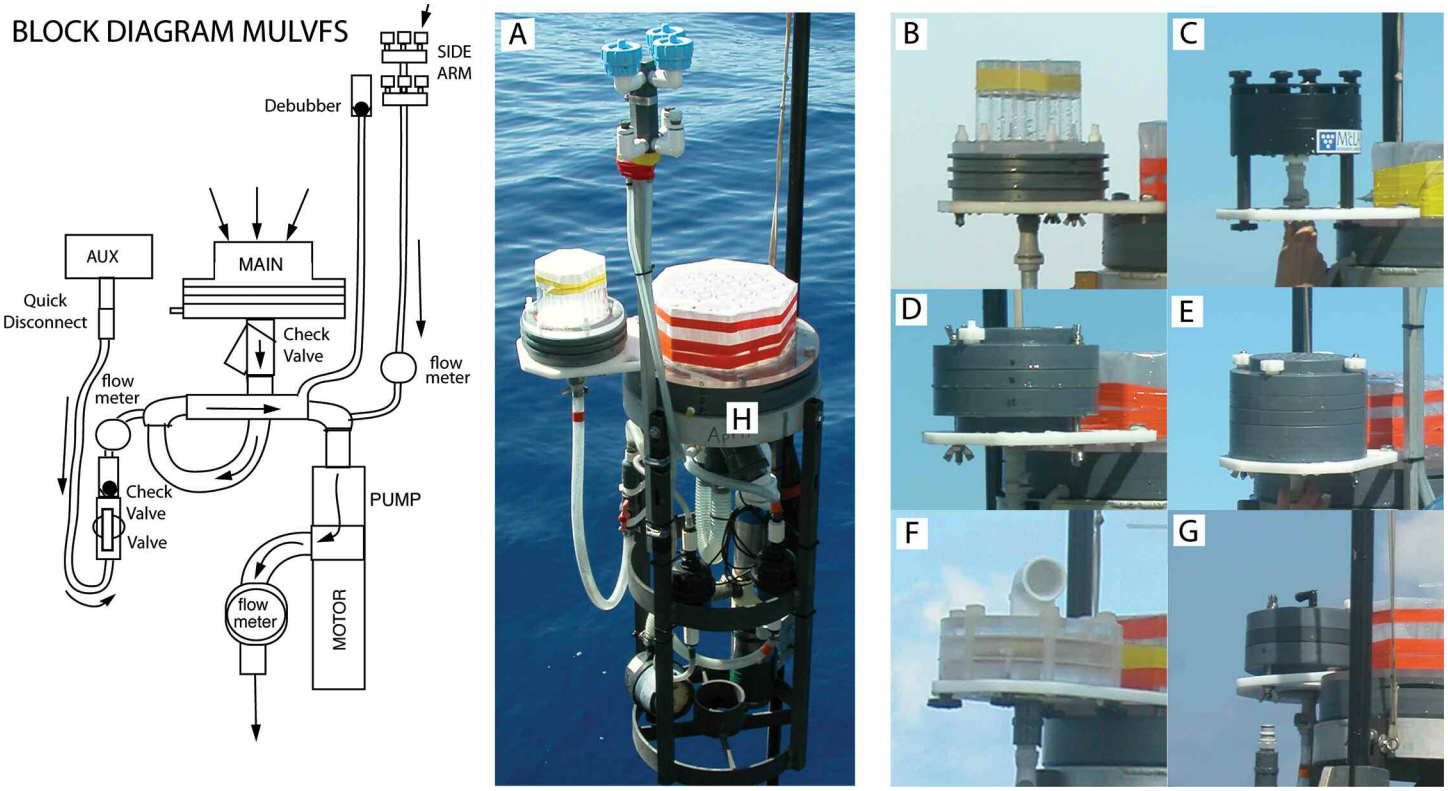

Fig. 1. Block flow schematic diagram and photograph of a MULVFS pump and filter holders used. (A) MULVFS configuration used during GEOTRACES expeditions and (B-G) pictures of 142 mm holders on auxiliary (AUX) flow path and main 293 mm holder (MAIN) (H). The 142 mm holders are B) mini-MULVFS (type A2), (C) McLane (type B), (D) 2-stage ^{234}Th-style (type C1), (E) 3-stage ^{234}Th-style (type C2), (F) RAPPID (type D1), and (G) in-line ^{234}Th-style (type D2).

blank" filters are processed identically to real filters, and are used to correct all samples for adsorption and process blanks.

Field deployments

The second leg of the first intercalibration cruise (IC1-2, R/V *Knorr*: KN193-6) sailed from Bermuda to Norfolk, VA in July 2008, with two MULVFS sampling stations: the Bermuda Atlantic Time Series (BATS) site at 31.8°N, 64.1°W in the oligotrophic Sargasso Sea, and a mesotrophic station at 37.0°N, 74.4°W in the slope water close to the north wall of the Gulf Stream. The second intercalibration cruise (IC2, KN195-8) sailed from Honolulu, HI to San Diego, CA in May 2009, again with two MULVFS sampling stations: the SAFe site at 30.0°N, 141.0°W at the edge of the oligotrophic North Pacific subtropical gyre, and a mesotrophic coastal station at 34.27°N, 120.04°W in the Santa Barbara Basin. Calm conditions prevailed during both expeditions.

MULVFS was deployed four times over the course of a week at both BATS and SAFe locations (Table 1). The first two casts at each station were devoted primarily to assessing filter holder design using the standard MULVFS QMA filter suite, described below. The third and fourth casts at each station were devoted to assessing flow-rate dependent effects on sampling and the sampling mechanics of different filter types. Two more casts were obtained in more particle-rich coastal waters during each expedition, with the first being filter holder design tests and second filter type tests. We focus much of our discussion on samples from low particle concentration oligotrophic waters where we deployed MULVFS multiple times and cast-to-cast hydrographic variability was lower than at the mesotrophic sites.

Due to calm weather conditions and low currents at BATS, MULVFS sample depths were always within a meter or two of wire out depths. Sampling depths were less than 7 m shallower than wire out depths at the Slope Water station, consistent with a minor influence from the nearby Gulf Stream. Similarly IC2 MULVFS sample depths were at nominal wire out depths at both SAFe and Santa Barbara Basin locations (Table 1), again a result of calm conditions. Pumps were spaced 25-50 m apart in the upper 250 m, and 100-200 m apart from 250-1000 m. Because MULVFS had to be deployed over the stern of R/V *Knorr*, the shallowest sample was chosen to be in a layer of near uniform particle concentration (based on particle optics) while remaining out of the immediate influence from the ship's propulsion system. Shallowest sampling depths were 30 and 20 m at BATS and the Slope water station, respectively, during IC1 and at 20 and 10 m at SAFe and SBB, respectively, during IC2.

Timing of sampling was different between the IC1 and IC2 cruises. During IC1, filtration sampling took place from

Table 1. MULVFS cast information during both intercalibration cruises. Columns are depth of pumps, volume and filter type through the main flow path, volume, filter holder type, and filter type through the auxiliary flow path, and volume and filter type through the side arm flow path. Descriptions of filter types and holder types are in tables 2 and 3, respectively.

Depth (m)	Main vol. (L)	Main filter type	Aux vol. (L)	Aux holder type	Aux filter type	Side-arm vol. (L)	Side-arm filter type
GEOTRACES IC1, KN193-6, 29 Jun 08-12 Jul 08, Bermuda to Norfolk, VA							
MULVFS Cast 1, BATS, 31.78°N, 64.1°W, 30 Jun 08 22:45-1 Jul 08 03:15 (UTC), (19:45-00:15 local), Event 79							
29	2,841	P,150/QMA^2,150	662	B2	P,150/QMA^2,150	11.2	s4
54	3,190	P,150/QMA^2,150	806	B1	P,150/QMA^2,150	12.1	s4
79	4,635	P,150/QMA^2,150	1,047	B2	P,150/QMA^2,150	20.3	s4
103	7,692	P,150/QMA^2,150	1,755	B2	P,150/QMA^2,150	53.4	s4
153	10,888	P,150/QMA^2,150	2,186	B2	P,150/QMA^2,150	71.4	s4
202	10,522	P,150/QMA^2,150	2,060	B2	P,150/QMA^2,150	59.8	s4
252	11,374	P,150/QMA^2,150	2,179	D1	P,150/QMA^2,150	65.6	s4
401	13,489	P,150/QMA^2,150	2,224	C2	P,150/QMA^2,150	71.3	s4
573	13,080	P,150/QMA^2,150	2,345	C1	P,150/QMA^2,150	82.6	s4
771	12,225	P,150/QMA^2,150	2,116	C2	P,150/QMA^2,150	63.8	s4
870	13,079	P,150/QMA^2,150	2,036	C1	P,150/QMA^2,150	59.8	s4
920	13	P,150/QMA^2,150	23	C1	P,150/QMA^2,150	0.0	s4
MULVFS Cast 2, BATS, 31.76°N, 64.1°W, 2 Jul 08 08:40 – 2 Jul 08 13:10 (UTC), (05:40-10:10 local), Event 92*							
30	3,290	P,150/QMA^2,150	743	C2	P,150/QMA^2,150	13.3	s4
55	3,685	P,150/QMA^2,150	0	C1	P,150/QMA^2,150	10.3	s2
80	4,908	P,150/QMA^2,150	1,004	D1	P,150/QMA^2,150	12.1	PC4/s4
105	10,584	P,150/QMA^2,150	1,466	D2	P,150/QMA^2,150	56.3	s4
155	10,359	P,150/QMA^2,150	1,882	C2	P,150/QMA^2,150	47.0	s2
205	11,029	P,150/QMA^2,150	1,701	B1	P,150/QMA^2,150	24.1	PC4/s4
255	12,157	P,150/QMA^2,150	1,522	B2	P,150/QMA^2,150	70.1	s4
330	13,365	P,150/QMA^2,150	1,781	B2	P,150/QMA^2,150	31.9	s2
480	14,086	P,150/QMA^2,150	1,429	B2	P,150/QMA^2,150	26.5	PC4/s4
680	12,867	P,150/QMA^2,150	1,669	B2	P,150/QMA^2,150	70.1	s4
830	12,847	P,150/QMA^2,150	1,094	B2	P,150/QMA^2,150	30.2	s2
930	9	P,150/QMA^2,150	17	D1	P,150/QMA^2,150	0.0	PC4/s4
MULVFS Cast 3, BATS, 31.75°N, 64.1°W, 4 Jul 08 08:40–4 Jul 08 13:10 (UTC), (05:40-10:10 local), Event 111							
30	3,047	P,150/QMA^2,150	740	C1	P,150/QMA^2,150	12.9	s4
55	3,326	P,150/QMA^2,150	217	B2	P,150/s4	12.7	s4
80	5,126	P,150/QMA^2,150	829†	B2	P,150/s8^2	23.6	s4
105	7,954	P,150/QMA^2,150	595	C2	P,150/s4	50.5	s4
155	10,396	P,150/QMA^2,150	2,208	C1	P,150/QMA^2,150	61.5	s4
205	10,505	P,150/QMA^2,150	1,952	B3	QMA^2,150‡	58.6	s4
255	11,500	P,150/QMA^2,150	2,258	B4	150/QMA^2,150§	67.3	s4
405	14,005	P,150/QMA^2,150	918	B2	P,150/s4	74.3	s4
580	14,491	P,150/QMA^2,150	877	C2	P,150/s8^2	83.9	s4
780	12,682	P,150/QMA^2,150	2,077	C1	P,150/QMA^2,150	70.7	s4
880	12,968	P,150/QMA^2,150	869	B2	P,150/s4	69.9	s4
930	–3	P,150/QMA^2,150	3	D1	P,150/s8^2	0.0	s4
MULVFS Cast 4, BATS, 31.73°N, 64.1°W, 5 Jul 08 21:24 – 6 Jul 08 01:54 (UTC), (18:24-22:54 local), Event 120							
30	2,933	P,150/QMA^2,150	2,147	〃		12.3	s4
55	1,442	P,150/S8^2,150	2,408	〃		58.0	QMA^2
80	1,632	P,150/S4,150	2,738	〃		28.0	s4
105	3,836	P,150/S8^2,150	2,640	〃		151.7	QMA^2
155	3,417	P,150/S4,150	2,693	〃		68.9	s4

continued…

Table 1. Continued

Depth (m)	Main vol. (L)	Main filter type	Aux vol. (L)	Aux holder type	Aux filter type	Side-arm vol. (L)	Side-arm filter type
205	9,288	P,150/QMA²,150	2,098	B3	P,150/QMA²,150	192.0	QMA²
255	5,295	P,150/S8²,150	2,757	〃		82.6	s4
330	5,209	P,150/S4,150	2,392	〃		249.0	QMA²
480	4,508	P,150/S8²,150	2,844	〃		102.5	s4
679	4,933	P,150/S4,150	2,541	〃		234.3	QMA²
829	5,139	P,150/S8²,150	2,457	〃		113.4	s4
929	–14	P,150/S4,150	1			0.0	QMA²
MULVFS Cast 5, Slope, 37.02°N, 74.41°W, 9 Jul 08 23:42 – 10 Jul 08 03:42 (UTC), (20:42-00:42 local), Event 130							
23	3,395	P,150/QMA²,150	826	B2	P,150/QMA²,150	3.4	s4
48	2,736	P,150/QMA²,150	715	B4	P,150/QMA²,150	12.3	s4
73	5,471	P,150/QMA²,150	1,261	B2	P,150/QMA²,150	40.9	s4
98	6,851	P,150/QMA²,150	1,587	B3	P,150/QMA²,150	52.3	s4
148	8,158	P,150/QMA²,150	1,697	B2	P,150/QMA²,150	51.5	s4
198	7,641	P,150/QMA²,150	1,694	B2	P,150/QMA²,150	50.6	s4
248	7,637	P,150/QMA²,150	1,658	C2	P,150/QMA²,150	51.6	s4
323	7,907	P,150/QMA²,150	1,730	C1	P,150/QMA²,150	46.1	s4
398	8,985	P,150/QMA²,150	1,830	C2	P,150/QMA²,150	58.4	s4
573	8,648	P,150/QMA²,150	1,686	C1	P,150/QMA²,150	53.6	s4
873	8,289	P,150/QMA²,150	1,661	C1	P,150/QMA²,150	162.3	s4
923	19	P,150/QMA²,150	25	D1	P,150/QMA²,150	–0.1	s4
MULVFS Cast 6, Slope, 37.02°N, 74.41°W, 10 Jul 08 23:30 – 11 Jul 08 03:30 (UTC), (19:30-23:30 local), Event 138							
23	3,861	P,150/QMA²,150	565	C2	P,150/s8	13.4	s4
48	3,379	P,150/QMA²,150	369	B5	P,150/s8	15.5	s4
98	7,331	P,150/QMA²,150	572	B2	P,150/s8	49.5	s4
148	8,228	P,150/QMA²,150	1,125	C1	P,150/s8	62.9	s4
198	8,894	P,150/QMA²,150	837	C2	P,150/s4	59.9	s4
273	7,239	P,150/QMA²,150	654	C1	P,150/s4	no	mf
348	8,772	P,150/QMA²,150	947¶	C1	P,150/s8²	56.9	s4
423	9,138	P,150/QMA²,150	617	B3	P,150/s4	52.5	s4
523	9,323	P,150/QMA²,150	630	B2	P,150/s8³	62.5	s4
623	7,352	P,150/QMA²,150	1,013	B2	P,150/s4	no	mf
773	7,757	P,150/QMA²,150	712	B2	P,150/s8²	169.0#	s4
873	(19)	P,150/QMA²,150	2	D1	P,150/s4	0.0	s4
GEOTRACES IC2, KN195-8, 6 May 09 – 29 May 09, Honolulu, HI to San Diego, CA							
MULVFS Cast 7, SAFe, 30.00°N, 141.00°W, 12 May 09 01:55 – 12 May 09 06:25 (UTC), (15:55-20:25 local), Event 2025							
20	3,701	P,150/QMA²,150	924	B2	P,150/QMA²,150	82.0	QMA²
45	3,915	P,150/QMA²,150	1,016	B2	P,150/QMA²,150		QMA²
70	4,542	P,150/QMA²,150	1,169	B2	P,150/QMA²,150	101.9	QMA²
95	5,551	P,150/QMA²,150	1,450	B2	P,150/QMA²,150	126.5	QMA²
120	6,623	P,150/QMA²,150	1,667	B2	P,150/QMA²,150	147.8	P,150/QMA²
170	9,258	P,150/QMA²,150	1,863	A2	P,150/QMA²,150	191.3	QMA²
220	11,392	P,150/QMA²,150	2,097	A2	P,150/QMA²,150	202.5	QMA²
345	12,156	P,150/QMA²,150	1,985	A2	P,150/QMA²,150	183.3	QMA²
495	11,887	P,150/QMA²,150	2,096	A2	P,150/QMA²,150	226.2	QMA²
695	12,949	P,150/QMA²,150	2,038	A2	P,150/QMA²,150	164.5	QMA²
845	12,162	P,150/QMA²,150	1,885	A2	P,150/QMA²,150	247.7	QMA²
945	–6	S4,150/P,150/ QMA²,150	-	A2	s4,150/P,150/ QMA²,150	0.0	QMA²

continued…

Table 1. Continued

Depth (m)	Main vol. (L)	Main filter type	Aux vol. (L)	Aux holder type	Aux filter type	Side-arm vol. (L)	Side-arm filter type
MULVFS Cast 8, SAFe, 30.00°N, 141.00°W, 14 May 09 02:58 – 14 May 09 07:26 (UTC), (16:58-21:26 local), Event 2041							
20	3,590	P,150/QMA^2,150	825	A2	P,150/QMA^2,150	19.8	s4
45	3,902	P,150/QMA^2,150	852	A2	P,150/QMA^2,150		s4
70	4,440	P,150/QMA^2,150	941	A2	P,150/QMA^2,150	22.7	s4
95	5,488	P,150/QMA^2,150	1,211	A2	P,150/QMA^2,150	29.6	s4
120	6,101	P,150/QMA^2,150	1,401	A2	P,150/QMA^2,150	34.8	s4
170	9,527	P,150/QMA^2,150	2,211	B2	P,150/QMA^2,150	63.1	s4
220	11,638	P,150/QMA^2,150	2,368	B2	P,150/QMA^2,150	74.6	s4
345	11,911	P,150/QMA^2,150	2,012	A2	P,150/QMA^2,150	63.8	s4
495	12,264	P,150/QMA^2,150	2,322	B2	P,150/QMA^2,150	79.0	s4
695	13,025	P,150/QMA^2,150	2,232	B2	P,150/QMA^2,150	74.8	s4
845	20	P,150/QMA^2,150	2	B2	P,150/QMA^2,150	0.0	s4
945	–3	P,150/QMA^2,150	0	A2	P,150/QMA^2,150	0.0	s4^2
MULVFS Cast 9, SAFe, 30.00°N, 141.00°W, 17 May 09 02:42 – 17 May 09 07:12 (UTC), (16:42-21:12 local), Event 2063							
20	1,629	P,150/S8^2,150	252	A2	P,150/s4^3	17.4	s4
45	1,536	P,150/S8^2,150	261	A2	P,150/s4^2		s4
70	4,597	P,150/QMA^2,150	529	A2	P,150/s8^2	23.6	s4
95	2,873	P,150/S8^2,150	426	A2	P,150/s4	33.9	s4
120	3,398	P,150/S8^2,150	371	A2	P,150/s4^3	46.6	s4
170	4,986	P,150/S8^2,150	604	A2	P,150/s4^2	68.0	s4
220	5,242	P,150/S8^2,150	1,090	A2	P,150/s4	83.9	s4
345	12,603	P,150/QMA^2,150	1,075	A2	P,150/s8^2	60.9	s4
495	5,130	P,150/S8^2,150	564	B2	P,150/s4^3	101.2	s4
695	5,386	P,150/S8^2,150	605	B2	P,150/s4^2	95.8	s4
845	4,993	P,150/S8^2,150	1,189	B2	P,150/s4	92.6	s4
945	–3	S4,150/P,150/ P,150/S8^2,150	0	A2	s4,150/P,150/s4^2,150	0.0	s4^2
MULVFS Cast 10, SAFe, 30.00°N, 141.00°W, 19 May 09 03:10 – 19 May 09 07:40 (UTC), (17:10-21:40 local), Event 2076							
20	908	P,150/S4^2	256	A2	P,150/mf^3	24.2	mf
45	3,626	P,150/QMA^2,150	290	A2	P,150/mf^2	25.7	mf
70	1,142	P,150/S4^2	165	A2	P,150/s2,mf^2	28.5	mf
95	1,046	P,150/S4^2	189	A2	P,150/s2,s4^3	40.8	mf
120	1,826	P,150/S4^2	485	B2	P,150/mf^3	42.7	mf
170	2,772	P,150/S4^2	825	B2	P,150/mf^2	79.5	mf
220	2,943	P,150/S4^2	365	A2	P,150/s2,mf^2	99.0	mf
345	2,719	P,150/S4^2	318	A2	P,150/s2,s4^2	86.9	mf
495	12,993	P,150/QMA^2,150	636	A2	P,150/mf^3	89.0	mf
695	2,566	P,150/S4^2	821	A2	P,150/mf^2	100.7	mf
845	2,445	P,150/S4^2	322	A2	s2, P,150/mf^2	97.2	mf
945	–5	S4,150/P,150/ S4^2,150	0	B2	s2,P,150/mf^2	0.0	mf^2
MULVFS Cast 11, Santa Barbara Basin, 34.27°N, 120.04°W, Cast 11.1: 24 May 09 22:54 – 25 May 09 01:54; Cast 11.2: 25 May 09 2:54 – 25 May 09 05:54 (UTC), (15:54-18:54; 19:54-22:54 local), Event 2110							
10**	1,141	P,150/QMA^2,150	255	A2	P,150/QMA^2,150	6.3	s4
60**	2,148	P,150/QMA^2,150	507	A2	P,150/QMA^2,150	20.8	s4
110**	2,745	P,150/QMA^2,150	625	A2	P,150/QMA^2,150	24.9	s4
160**	2,952	P,150/QMA^2,150	704	A2	P,150/QMA^2,150	29.2	s4
30	1,895	P,150/QMA^2,150	212	A2	s2/P,150/QMA^2,150	16.9	s4
130	2,463	P,150/QMA^2,150	647	A2	P,150/QMA^2,150	16.5	s4
230	3,052	P,150/QMA^2,150	753	A2	P,150/QMA^2,150	30.1	s4

continued…

Table 1. Continued

Depth (m)	Main vol. (L)	Main filter type	Aux vol. (L)	Aux holder type	Aux filter type	Side-arm vol. (L)	Side-arm filter type
330	3,498	P,150/QMA^2,150	326	A2	s2/P,150/QMA^2,150	26.8	s4
430	3,278	P,150/QMA^2,150	774	A2	P,150/QMA^2,150	38.1	s4
480	3,529	P,150/QMA^2,150	863	A2	P,150/QMA^2,150	33.0	s4
530	2,668	P,150/QMA^2,150	329	A2	s2/P,150/QMA^2,150	32.4	s4
380	–3	S4,150/P,150/ QMA^2,150	0	B2	s2/P,150/QMA^2,150	0.0	s4^2
MULVFS Cast 12, Santa Barbara Basin, 34.27°N, 120.04°W, Cast 12.1: 26 May 09 22:50 – 27 May 09 01:50; Cast 11.2: 27 May 09 2:54 – 27 May 09 05:54 (UTC), (15:50-18:50; 19:54-22:54 local), Event 2125							
10**	223	P,150/S4	69	A2	P,150/s4^2	5.8	s4
60**	1,144	P,150/S8^2	151	A2	P,150/s2,s8^2	22.5	s4
110**	928	P,150/S4	234	A2	P,150/s4^2	21.5	s4
160**	2,592	P,150/QMA^2,150	170	A2	P,150/s2,QMA^2,150	24.6	s4
30	0	P,150/QMA^2,150	0	A2	P,150/s2,QMA^2,150	0.0	s4
130	1,548	P,150/S8^2	257	A2	P,150/s4^2	23.5	s4
230	1,822	P,150/S8^2	172	A2	P,150/s2,s4^2	29.8	s4
330	1,074	P,150/S4	305	A2	P,150/s4^2	26.0	s4
430	1,205	P,150/S4	298	A2	P,150/s4^2	39.3	s4
480	3,653	P,150/QMA^2,150	265	A2	s2,P,150/QMA^2	34.6	s4
530	1,642	P,150/S8^2	165	A2	P,150/s2,s4^2	33.3	s4
380	0	S4,150/P,150/S8^2	-	B2	s2,P,150/s4^2	0.0	s4^2

*In-line Mn/Fe cartridges installed below all auxiliary holders.
†Flow volume and photo of auxiliary s8 filters indicate partial flow bypass, prefilter sealed properly.
‡No 51 µm prefilter loaded.
§Only 150 µm support loaded.
‖In-line cartridge prefilter/adsorber on auxiliary channel except at 205 m.
¶Filter bypass.
#Broken side-arm holder.
**Second cast

~18:30 to 25:00 (dusk) local time, or from 6:00 to 10:30 (dawn) (Table 1) to maximize contrast of particle concentration in the euphotic zone (Bishop and Wood 2008). During IC2, filtration was timed consistently for the mid-afternoon (local time) to minimize diurnal variability of particle concentration (Table 1). Pumping duration was 4.5 h at BATS and SAFe and 4 and 3 h, respectively, in the relatively particle rich waters of the Atlantic Slope Water and Santa Barbara Basin. Vacuum (0.5 atm) was used to draw excess water from main and auxiliary samples beginning at the time each pump was being removed from the wire. The procedure continued on deck until deemed complete. Samples from below 100 m were drained easily within minutes; those from the euphotic layer sometimes took 10-30 min.

Filter type descriptions

Here, our goals were to assess the sampling mechanics associated with a variety of micron and sub-micron filter types (Table 2). The standard MULVFS QMA filter suite ("P, 150/QMA^2,150") consists of a 51 µm polyester 33% open area mesh prefilter (SEFAR 07-51/33, "P") supported by a 37% open area 150 µm polyester mesh (SEFAR 07-150/37, "150"), followed by two identical Whatman QMA quartz fiber filters ("QMA^2") supported by a 150 µm polyester mesh (Bishop and Wood 2008). Whatman QMA filters have been used with MULVFS since 1991 (Bishop 1999). The nominal pore size of QMA filters is close to 1 µm. Since QMA filters are depth filters, deploying two QMA filters in series allows for a greater efficiency of particle capture, and thus a population of particles in the larger sub-micron class is collected on the second (or "bottom") filter (see Bishop and Edmond 1976). Nominal size fractions from the standard filter suite are thus > 51 µm, 1-51 µm, and <1 µm. The advantage of using the second identical filter in series is that information on the picoplankton size fraction is obtained in shallow waters while samples from sub-euphotic waters serve as a cross check on elemental blanks.

As the sampling characteristics of the standard MULVFS QMA filter suite are well known from over 20 years of MULVFS experience, this was the reference to which other filter types were compared, and the filter suite used for comparing different filter holder types.

QMA filters can be acid-leached and precombusted, and are thus well-suited for determinations of organics and organic isotopes (Bishop et al. 1999; Lam and Bishop 2007),

Table 2. Filter types, their nominal pore sizes, brands, and abbreviations used in the text.

Filter type	Nominal pore size (µm)	Brand used	Abbreviation used for deployment (single/paired/triple)	Nominal particle size fractions for single and paired filters (abbreviation)
Polyester prefilter	51 (33% open area)	Sefar PeCap	P/–/–	>51 µm
Polyester support filter	150 (37% open area)	Sefar PeCap	150/–/–	Used as support only
Quartz fiber filter	1	Whatman QMA	–/QMA[2]/–	Top: 1–51 µm (QT)
				Bottom: <1 µm (QB)
Polyethersulfone membrane	0.8	Pall Supor-800	S8/S8[2]/S8[3]	Top: 0.8-51 µm (S8T)
				Bottom: <0.8 µm (S8B)
	0.45	Pall Supor-450	S4/S4[2]/S4[3]	Top: 0.45-51 µm (S4T)
				Bottom: <0.45 µm (S4B)
	0.2	Pall Supor-200	S2/–/–	0.2–51 µm (S2)
Mixed cellulose acetate and cellulose nitrate	0.45	Millipore MF	MF/MF[2]/MF[3]	Top: 0.45-51 µm
				Bottom: <0.45 µm

acid-labile trace metals (Lam et al. 2006; Lam and Bishop 2008; Bishop and Wood 2008), and short-lived radionuclides (Buesseler et al. 2008). QMAs add complexity to the low level determination of aluminum and uranium since their dissolved phases adsorb strongly to quartz (Bishop unpubl. data). In many cases, QMAs are poorly suited to determinations of total particulate trace elements using strong digests containing hydrofluoric acid due to the high filter blank. We thus examined the in-situ pumping sampling characteristics of a variety of sub-micron filter types. We focused our assessment on polyethersulfone filters (Pall "Supor") and mixed cellulose acetate and cellulose nitrate filters (Millipore "MF"), two filter types known to have good flow characteristics. Track-etched polycarbonate membrane filters (e.g., Whatman "Nuclepore" filters) clog easily (filtering approximately 40% of the volume permitted by Supor or MF filters of similar pore size) and are thus not suitable for large volume in-situ filtration and were not tested in the main 293 mm or auxiliary 142 mm holders.

For mass balance purposes, particle collection would ideally complement the 0.2 µm capsule-filtered or 0.45 µm membrane-filtered seawater recommended for dissolved trace metal analysis on the US GEOTRACES program (GEOTRACES 2010). As with QMA filters, the efficiency of particle collection by Supor and MF filters is improved by increasing the effective depth of filter material. We thus tested 0.2 µm, 0.45 µm, and 0.8 µm Supor filters, deployed singly, serially in pairs, and occasionally serially in triplicate (Table 1).

Our assessments of sub-micron filter types were based on requirements for adequate volume throughput (i.e., the effect of pore size on filter flow rate), the need for even particle distribution across the filter to allow for subsampling, the need to accurately sample particle populations, and the practical need for ease of filter handling.

Filter holder descriptions

We tested several designs of 142 mm filter holders (Fig. 1B-G) and compared their particle distribution and retention characteristics to the standard 293 mm MULVFS filter holder (Bishop and Wood 2008). All filter holders that we tested allowed for in-situ separation of large and small particle size classes. All filter holders tested had a base plate with a porous polyethylene frit to support a small pore-sized filter (QMA, Supor, or Millipore MF), a prefilter support plate, and a top plate allowing for inflow; many incorporated some sort of baffle design intended to reduce turbulence and minimize particle loss. The main variations on this theme were the designs of the water intake; the prefilter support plate; and the baffle system for retaining particles, each of which we will examine in turn.

There were four main designs of holders that we tested (types A-D, Fig. 1B-H), each of which had variations within a type to test the effectiveness of specific features (Table 3).

The MULVFS filter holder (holder A1, Fig. 1H, Bishop and Wood 2008) has three anti-washout baffle systems designed to prevent particle loss: (1) a heavy polyethylene plastic film cover with incised triangular flaps, centered over (2) 52 hexagonally separated 2.2 cm ID baffle tubes that are 11 cm tall, and (3) a 1.25 cm thick square 1.25 cm polystyrene grid sitting only 1.5 mm off the surface of the prefilter (Bishop and Wood 2008). This square grid is also referred to as 'egg crate' in discussions below. This design has been validated in horizontal current flows of up to several hundred cm s^{-1} in the core of the Gulf Stream and shown to collect particles without any visible disturbance of sample (Bishop et al. 1985). All components except stainless steel filter holder bolts are plastic and are acid leached prior to use.

The mini-MULVFS holder (holder A2—Fig. 1B, Fig. 2) is simply a scaled down version of the main MULVFS holder, with the following modifications: a reduction in the number,

Table 3. Filter holder descriptions

Type	Code	Origin	Intake	Baffle style	Nr of stages	Prefilter support material	Reference
MULVFS	A1	Bishop	Vertical: 52 7/8-inch ID tubes	PE film cover, 11 cm tubes, eggcrate grid	4	Eggcrate grid	Bishop and Wood 2008
Mini-MULVFS	A2	Lam	Vertical: 32 1/2-inch ID tubes	PE film cover, 10 cm tubes, eggcrate grid	4	Eggcrate grid	This article
McLane, standard	B1	McLane	Horizontal: Large radial intakes	2.5 cm long honeycomb Ti baffle	3	Stainless steel mesh	Morrison et al. 2000
McLane, all-plastic	B2	McLane	Horizontal: Large radial intakes	2.5 cm long honeycomb plastic baffle	3	Perforated polypropylene	Modification of standard McLane for trace metal applications
McLane, mix	B3	McLane	Horizontal: Large radial intakes	2.5 cm long honeycomb plastic baffle	3	Stainless steel mesh	Modification of standard McLane
McLane, mix	B4	McLane	Horizontal: Large radial intakes	2.5 cm long honeycomb Ti baffle	3	Perforated polypropylene	Modification of standard McLane
McLane, all-plastic	B5	McLane	Horizontal: Large radial intakes	5 cm long honeycomb plastic baffle	3	Perforated polypropylene	Modification of standard McLane
"^{234}Th-style," 2-stage	C1	Buesseler	Vertical: 69 1 cm diameter holes	3.8 cm long	3	Eggcrate grid	Buesseler et al. 1995
"^{234}Th-style," 3-stage	C2	Moran	Vertical: 69 1 cm diameter holes	3.8 cm long	4	Eggcrate grid	Same as ^{234}Th 2-stage, but with an additional stage
RAPPID	D1	Sherrell	Single PVC intake elbow, 15.2 cm^2 orifice	No baffles	3	Eggcrate grid	Sherrell 1991; Sherrell and Boyle 1992
"^{234}Th-style," 2-stage, inline	D2	Buesseler	Single nylon barbed elbow, 0.64 cm^2 orifice	No baffles	3	Eggcrate grid	Modification of ^{234}Th-style 2-stage for in-line filtration

diameter, and length of tube baffles, to 32 hexagonally spaced 1.25 cm ID tubes that are 10 cm tall; the addition of O-rings between the plates to improve the simplicity of getting a reliable filter seal on membrane filters; the ability to remove the filter holder from the pump without loosening the seal holding the plates together (a feature of McLane pump filter holders), and the replacement of stainless steel threaded bolts by threaded studs made of acetal plastic. Its effective filtration area is 125 cm^2, approximately one quarter of the 506.7 cm^2 effective filtration area of the main-MULVFS filter holder. All components are plastic and can be acid-leached prior to use.

Filter holders B (McLane holders; Fig. 1C) and D (elbow inlet style, Figs. 1F and G) were constructed with a solid top with the aim that the holder does not act as a sediment trap or collect additional particles as the pump is raised through the water column during recovery (Sherrell 1991). Bishop et al. (1986) reported this effect to be small, although some large particles are found on MULVFS blank prefilters; such particles likely arrive during the initial deployment of the pump when surface water floods the filters than upon recovery since typical flow meter values for blank filters are several liters compared with thousands. Water intake for holder B is through large radial openings that feed the flow down through a 2.5 cm long honeycomb baffle made of titanium in the standard model (B1) (Morrison et al. 2000), and plastic in the trace-metal model (B2). This baffle is designed to straighten the flow and suppress turbulence, and distribute particles evenly across the filter. The prefilter support plate is a 316 stainless steel mesh in the standard model (B1) and a perforated polypropylene disc with 40% open area in the trace-metal model (B2). We additionally mixed and matched the baffle and prefilter support plates (type B3, B4), and also tried a model with a longer baffle (type B5) (Table 3).

Filter holders C1 (Fig. 1D) and C2 (Fig. 1E) have vertical intakes that are 69 equally spaced 1-cm diameter holes drilled in concentric circles through the top PVC plate, quite similar in concept to early filter holders used on the Large Volume in-situ Filtration System (Bishop and Edmond 1976), which carried a single filter holder and sampled one depth per deployment. These baffle holes were intended to dis-

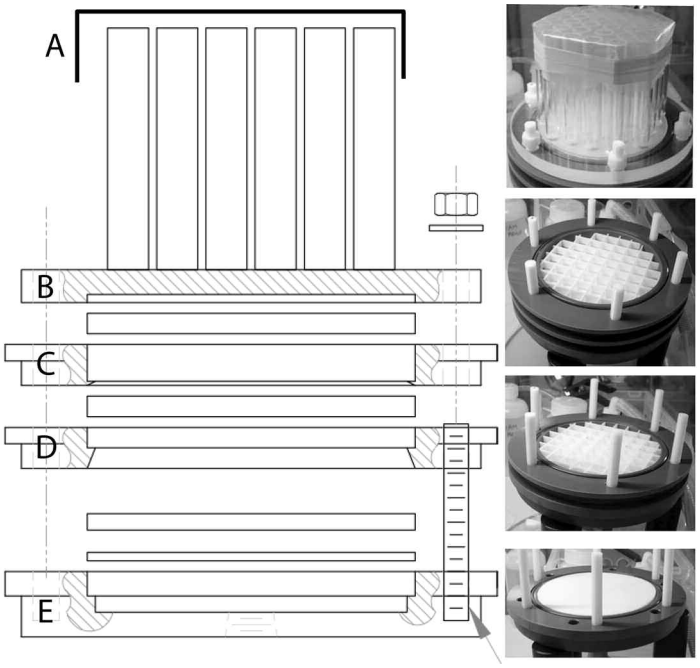

Fig. 2. Schematic of mini-MULVFS holder (Fig. 1B, type A2) with pictures of the baffle and filter support plates. The baffle logic follows that of the main MULVFS filter holder (Bishop and Wood 2008) with modifications to facilitate mounting on McLane pumps and handling in the laboratory.

tribute particles evenly across the filter surface and protect particles from washing off the prefilter during pump retrieval (Buesseler et al. 1995). The top PVC plate is 5 cm thick, with the 3.8 cm long baffles opening up into a 1.2 cm tall open space above the prefilter. The C-type holders have been used extensively by the ^{234}Th community to collect size-fractionated particles for determination of POC export.

The top plates of holder types D are sealed, and water intake is through a single intake elbow centered in the top plate with horizontally facing orifice. The cross-sectional area of the intake orifice for holder D1 (Fig. 1F) is 15.2 cm^2 and feeds a flow expansion chamber (Sherrell 1991), and is only 0.6 cm^2 for holder D2 (Fig. 1G). Holder D2 is a modification of the C-type holders meant for on-deck in-line filtration rather than in-situ filtration. We deployed it to compare to holder D1 as an experiment to test the effect of orifice size on particle collection.

Imaging of filters

We used controlled illumination photography at sea to quantitatively document the performance of different filter holders and filter types for the amount and evenness of distribution of particles on the filters (Lam and Bishop 2007). Briefly, filters were dried at 60°C and imaged at constant light, fixed focal distance, focus, and camera settings (shutter speed, ISO, white balance, f-number). An absolute optical density calibration of image data were achieved by photographing a white target (the dull side of a 293 mm diameter 0.45 µm pore size Supor filter) under identical conditions. Although lighting intensity varied by 20% across our images of 293 mm filters and by several percent across zoomed images of the center of filters, it was possible to "flatten" or compensate for this variation by normalizing images using the variations of optical density of the white target imaged under identical lighting conditions. We used images of in-situ blank filters as optical density "0" reference as described by Lam and Bishop (2007). Calibration of the flattened red, green, blue (RGB) counts to optical density was achieved by imaging the white target at increasingly fast shutter speeds. We then computed filter area and flow volume normalized green (G) optical density of > 51 µm prefilter images as a photographic proxy for the relative > 51 µm particle concentration with depth (Lam and Bishop 2007).

We used ImageJ software version 1.41 (National Institutes of Health) to analyze evenness of filter loading on QMA, Supor, and MF filters. We also used the software to the measure size distributions of > 51 µm particles on selected MULVFS main and auxiliary samples. In the later analysis, the 25 µm native resolution of images was averaged to 50 µm to remove the effects of the 50 µm mesh on particle detection. Furthermore, "flattened" image RGB count values were scaled up using a linear scaling factor of ~1.25 to brighten but not saturate the images. The 24-bit RGB values were transformed to 8 bit (0-255) gray scale values and then processed for particle size. Particles were considered detected if the count of an individual pixel was below a threshold of 200 counts (relative to an average image intensity of ~220 counts). A particle was classified only if it was greater than 150 µm in size (an area greater than 8 pixels).

Chemical analyses of particles

Subsamples of each filter were leached at 60°C in 0.6N HCl overnight and analyzed by high-resolution inductively coupled mass spectrometry (HR-ICP-MS) according to methods described in Bishop and Wood (2008). For > 51 µm particles, subsamples representing 2% of the 293 mm filters and 10% of the 142 mm filters were analyzed. For < 51 µm particles, subsamples representing 2.5% of the 293 mm filters and ~10% of the 142 mm filters were analyzed. The entire side arm filter was analyzed in most cases. Elements determined were Li*, Na, Mg*, Al, P, K*, Ca*, Cr, Mn, Fe, Co, Ni, Cu, Zn, Rb, Sr*, Y, Cd, I, Cs, Ba, Tl, Pb, Bi, Ce, Nd, and U*. Elements marked with asterisks (*) were corrected for seasalt components using Na (Bishop et al. 1977). Here we report the concentrations of elements where the recovery from a 0.6N HCl leach is 100% and where phase and particle size distribution associations are distinct (e.g., P and Cd - soft parts; Mn, Ba, Ca, Sr inorganic phases). For example, P and Cd are highest in near surface waters, whereas Mn and Ba are lowest in surface waters and highest at ~500 m. Sr was chosen because of its dominant association with > 51 µm Acantharia in the surface layer. Ca has a biotic source and occurs in both large and small particles. All reported concentrations have been corrected for process and adsorption blanks (Appendix: Table S1, Fig. S1).

We note that the blank levels of all filter types were significantly lower for the 2009 IC2 expedition in the Pacific compared with the 2008 IC1 expedition in the Atlantic. As these are "dipped blank" filters that were deployed to ~900 m on a disconnected pump, we attribute the lower blank levels during 2009 IC2 to the lower concentrations of most TEIs in the Pacific Basin compared with the Atlantic Basin. Repeat measurements of selected samples yielded relative standard deviations ranging from 2% to 12% for most filter types, and 10% to 41% for the bottom 0.8 µm Supor filter (Appendix: Table S2). Error bars in concentration profiles are the propagated standard deviations from the error associated with the blank samples (Appendix: Table S1), and the error from repeat measurements of the sample (Appendix: Table S2). At low concentrations, the uncertainty associated with the blank correction dominates. The assessment of filter blanks from total digests is addressed in Planquette and Sherrell (2012).

Assessment

Hydrographic and optical variability

Figs. 3 and 4 show profiles of particle beam attenuation coefficient (c_p), standard deviation of temperature, salinity, and potential density of grouped CTD-trace metal rosette profiles at BATS and SAFe, respectively. These data are plotted with turbidity (mFTU), temperature, and salinity (Appendix: Figs. S2 and S3). Because calm conditions prevailed during our occupation of the BATS and SAFe stations, mixed layers were shallower than 5 m and effects of turbulence induced by ship motion on particle sampling were minimal (Figs. 3c and 4c).

We used the statistics of density, temperature, and salinity (standard deviation at depths sampled) across casts as a metric of hydrographic variability and hence of inter-cast comparability. At BATS, minimum variability (or best hydrographic consistency) was found at depths between 150 and 400 m (Fig. 3b).

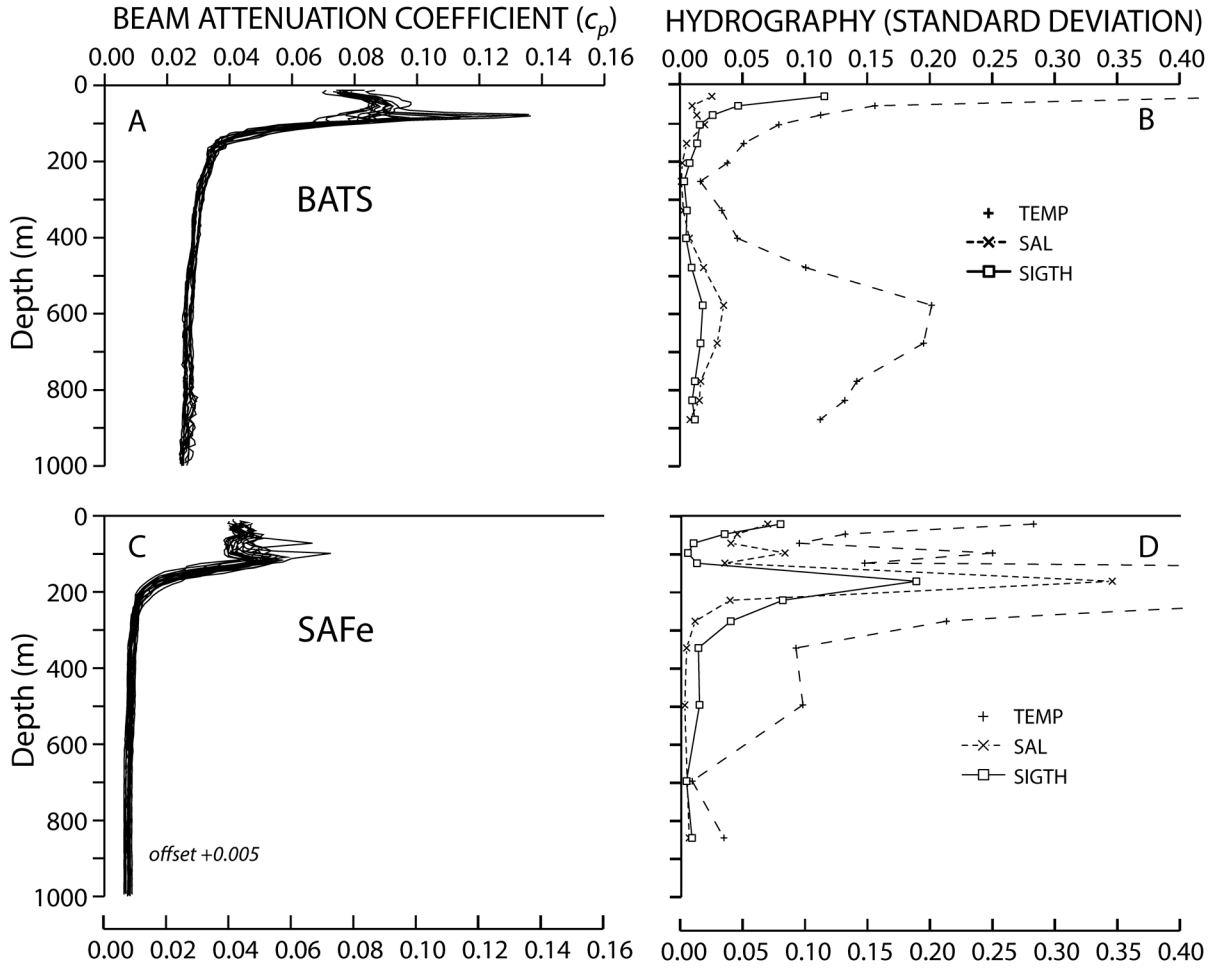

Fig. 3. Optics and hydrographic data from the Trace Metal CTD (Cutter and Bruland 2012) deployments during IC1 at the Bermuda Atlantic Time-Series Station (BATS) and during IC2 at the SAFe station (30°N 140°W). (A and C) Particle beam attenuation coefficient (c_p) at 660 nm from a WET Labs. C-Star transmissometer. (B and D) Standard deviation of temperature, salinity, and potential density anomaly. Least hydrographic variability was found between 200 and 400 m at BATS and deeper than 350 m at SAFe. Mixed layer depth at both locations was shallower than 5 m due to windless conditions. The data including temperature, salinity, density, and turbidity are shown in Supplemental Figs. S2 and S3, Appendix.

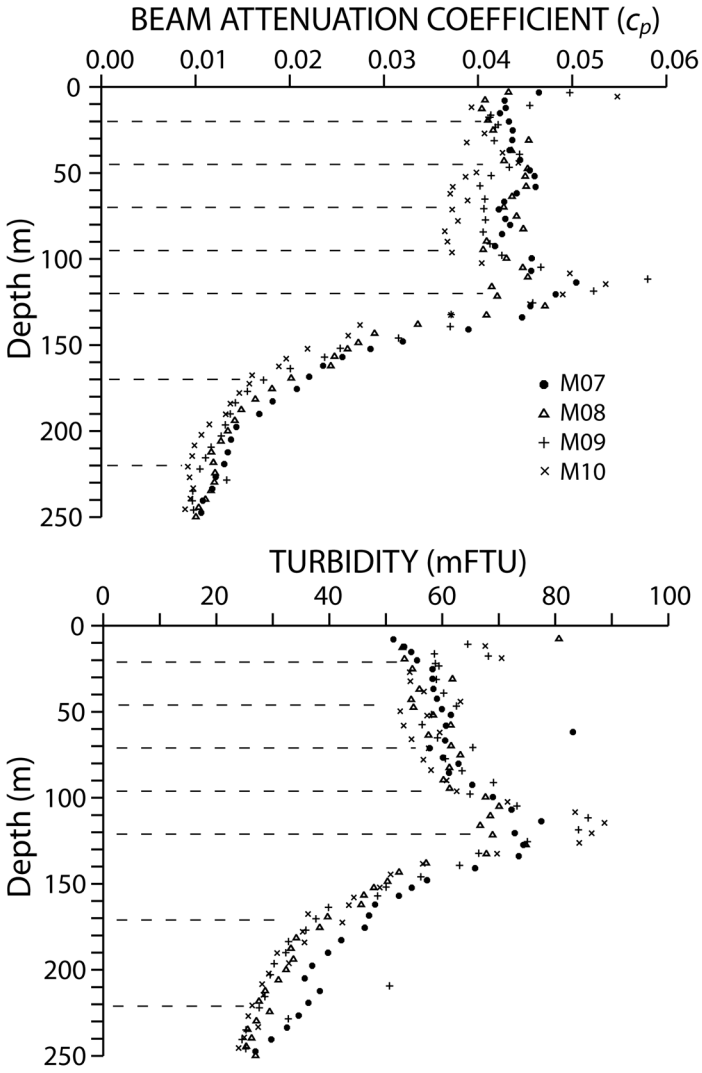

Fig. 4. Profiles of particle beam attenuation coefficient and turbidity deployed during MULVFS casts at SAFe. Light dashed lines denote MULVFS sampling depths. Although time of day was almost the same for each cast, hydrographic variability contributes from 10% to 20% to the concentration variability in the upper 200 m. Profiles M07 and M08 are almost identical.

Waters deeper than 1000 m (data not shown) exhibited greater temperature/salinity variation than at all depths shallower than 1000 m. At SAFe, there was progressive shoaling of the thermocline and halocline from 170 m to 120 m over the course of 10 d on station (Appendix: Fig. S3). Shallower waters exhibited far greater salinity and temperature excursions (including salinity compensated thermal inversions) compared with those encountered at BATS. Because of this, the density, temperature, and salinity standard deviations at sampled depths were highest near 170 m and remained generally high in shallower waters. At SAFe, the hydrographic variability was lowest at MULVFS sampling depths of 345 m, 495 m, 695 m, and 845 m, and minimal below 1000 m (Fig. 3d). In the discussion below, we focus on the three deepest sampled depths for cast-to-cast comparisons at SAFe where we study the effects of sample filtration flow rate on large particle retention.

At BATS, beam attenuation coefficient and turbidity profiles (Figs. 3a, Appendix: Fig. S3) showed elevated particle abundances in the upper 100-150 m consistent with the dominance of phytoplankton and other biogenic particle sources in the euphotic layer. Particle beam attenuation coefficient ranged by 10% to 15% in waters shallower than 50 m and was highly variable near the 100 m deep particle maximum, where values ranged by more than 50%. Below 150 m, particle concentrations decrease sharply and ranged less than 10%. Much of the concentration variability in waters shallower than 150 m was due to diurnal changes of the balance between phytoplankton primary production and zooplankton grazing; in oligotrophic waters, beam attenuation coefficient is highest in the late afternoon and lowest near dawn (Bishop and Wood 2008; see also Siegel et al. 1989).

At SAFe, concentrations were also highest in the upper 120 m but concentrations were at least 2-fold lower than at BATS at all depths (Fig. 3c), levels as low as we have ever observed. Beam attenuation coefficient data from multiple trace metal rosette casts varied over a range of 30% in shallow waters down to 120 m and ranged by 15% and 20% in deeper waters. These data reflect not only the hydrographic variability noted above but also the diurnal cycle of particle production and consumption.

MULVFS casts at SAFe were timed to occur during the same time of day to eliminate diurnal effects. Our optics data from these casts (Fig. 4) show that particle concentrations ranged by 10% to 15% from surface to 90 m, with variability of ~20% at the 110 m particle maximum and down to a depth of 250 m. Optics data suggest that MULVFS casts M07 and M08, which occurred 2 d apart, had nearly identical particle concentration profiles.

Sampled particle population by different (sub)-micron filter types

The multi-flow path configuration of each MULVFS pump allows for several filter types to be deployed simultaneously and compared directly. Depth profiles of the sum of particle concentrations from the three size fractions from the standard MULVFS QMA suite of filters (> 51 µm, 1-51 µm, <1 µm) are consistent with those collected simultaneously on the 0.45 µm Supor 47 mm side-arm filters deployed without prefilters (Fig. 5), demonstrating that the standard filter suite is closely sampling the total (or >0.45 µm) suspended particle population for Sr, Mn, and Ba throughout the water column. However, particulate phosphorus in the > 0.45 µm fraction is about 35% higher than the "standard" filter suite shallower than 120 m, consistent with the presence of small picoplankton and bacteria, some of which are missed by the standard QMA filter suite; below 300 m, the "standard" and > 0.45 µm P concentrations agree within 10%. The contribution of the bottom <1 µm filter varies by element and is greatest for P in near surface

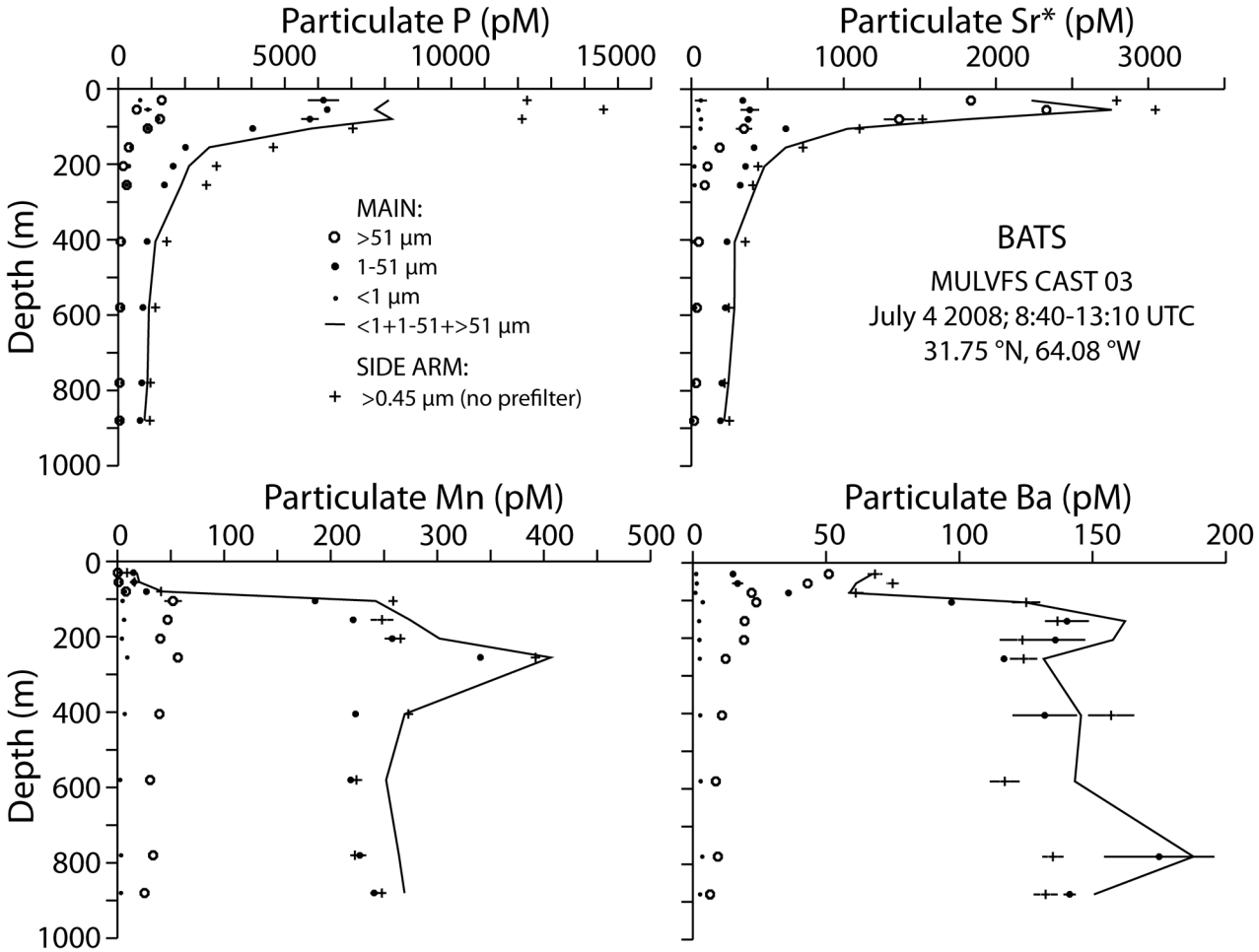

Fig. 5. Comparison of particle concentration profiles for P, Sr*, Mn, and Ba at the Bermuda Atlantic Time-Series (BATS) location during IC1. Sr* data are corrected for seasalt Sr. Data from the standard MULVFS filter suite polyester mesh (>51 µm size fraction) and paired QMA filters (1-51 and <1 µm size fractions), and the total of the three size fractions, are compared with the > 0.45 µm 'side arm' fraction. Side arm Sr*, Mn, and Ba closely agree with the sum of three standard filters fractions. Side arm P concentrations are ~40% higher in samples shallower than 100 m, denoting the presence of significant populations of living material below the 0.8 µm effective pore size cutoff of the paired QMA filters.

waters, again indicating partial collection of the picoplankton and bacterial communities. The > 51 µm size fraction dominates the distributions of total Sr* and Ba in waters shallower than 100 m. By contrast, both total P and Mn are dominated by < 51 µm particles. In deeper waters, all elements are dominant in the small (<51 µm) particle size fraction, and we focus on this fraction first.

To assess the sampled particle population by different submicron filter types, we use data from four MULVFS casts at the SAFe station during IC2 with different combinations of filter types on the main and auxiliary flow paths (Table 1). We focus on IC2 because we had better control of data quality and analysis blank. To assess the degree of variability that we should expect from other filter types between casts and between the main and auxiliary flow paths, we first compare suspended particulate (1-51 µm) profiles from the first two casts at SAFe (M7 and M8) in which the standard QMA suite of filters was loaded in all filter holders. Replication in the profiles of particulate P, Cd, Ba, and Mn collected on the standard QMA suite of filters between casts M7 and M8 and between the main and auxiliary flowpaths is very good (Fig. 6A), demonstrating that the two 142 mm filter holders used during IC2 (mini-MULVFS A2, McLane B2) work as well as the main MULVFS holder (A1) for collecting 1-51 µm particles. The only systematic difference is for Mn, where concentrations derived from the auxiliary flow path are systematically ~15% lower than those from the main flow path below 150 m. Hydrodynamic differences in filtration by main and auxiliary holders is ruled out as a cause for the Mn descrepency since main and auxiliary filters are supported by identical 149 µm porous polyethylene frit, are isolated by check valves, experience identical pressure differential due to connection to a common manifold above the pump, and their flow volumes are independently metered (Fig. 1A). The 15% difference appears to result from the 50% lower loading of the

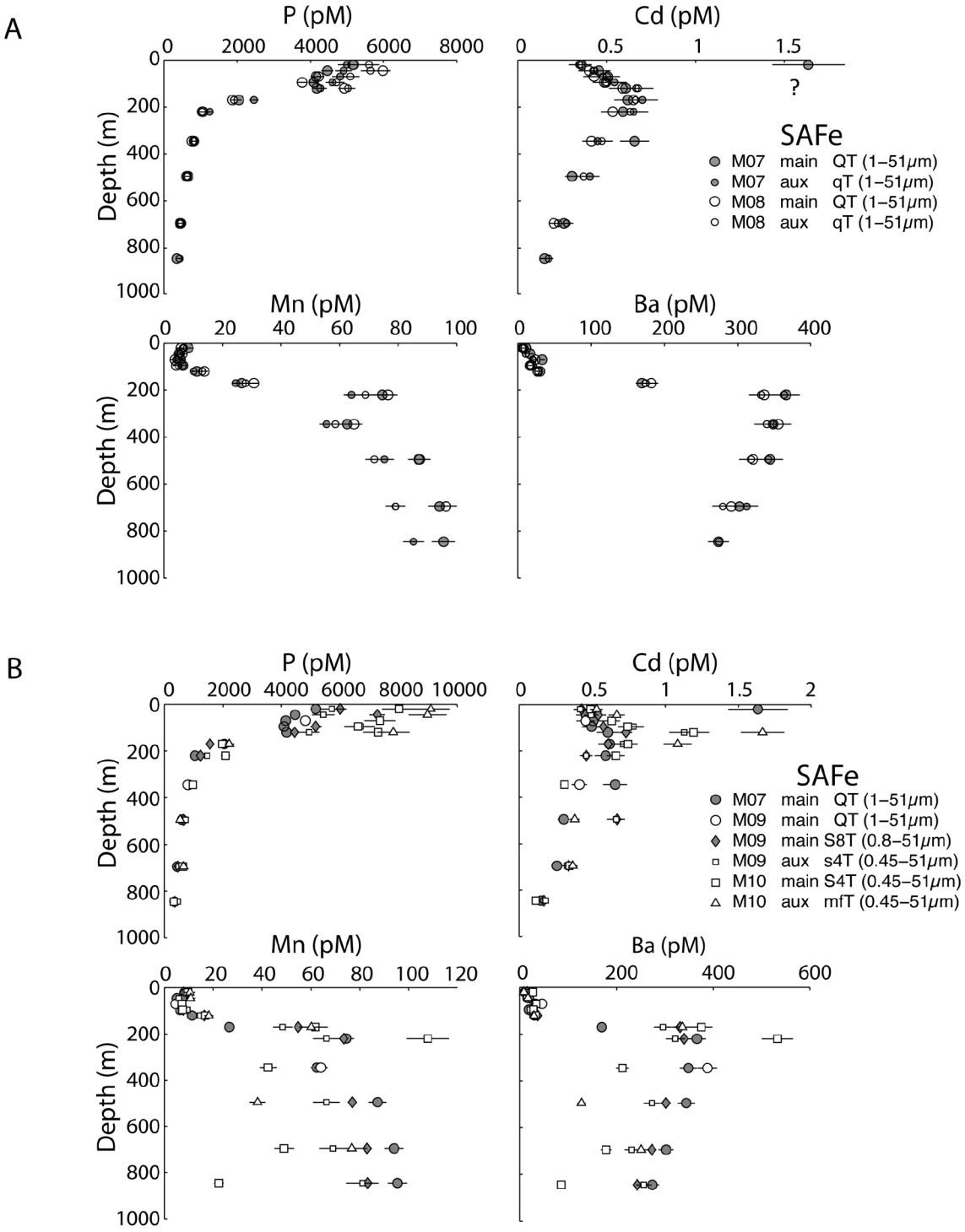

Fig. 6. (A) Comparisons of 1-51 μm profiles for particulate P, Cd, Mn, and Ba at SAFe during MULVFS casts M07 and M08 collected on paired QMA filters. Error bars are standard deviations propagated from replicate blanks and replicate subsamples. Data show close agreement of particle concentrations collected using main (type A1) and auxiliary filter holders (type A2, B2; Table 1). The ~15% Lower Mn in the auxiliary 142 mm flow path compared with main 293 mm data in waters below 200 m is likely due to 50% lower particle loading on auxiliary QMA filters, lowering the efficiency of collection of sub-micron Mn particles that pass through the first QMA filter. (B) Comparisons of particulate P, Cd, Mn, and Ba from the top filter of all micron and submicron filter types tested at SAFe on IC2: QMA (QT—M07, M09 main), 0.8 μm Supor (M09 main S8T), 0.45 μm Supor (M09 aux s4T and M10 main S4T), and 0.45μm MF (M10 aux mf). Euphotic zone concentrations of P and Cd are higher in the submicron filter types (Supor and MF) than QMA filters as expected, reflecting more efficient collection of submicron-sized picoplankton and bacteria. Below 200 m, concentrations of Mn and Ba are lower in the submicron filter types compared with QMA despite their lower nominal pore sizes. 0.8 μm Supors are best behaved of the submicron filter types.

auxiliary versus main filters at deeper depths, which causes a less efficient retention of sub-micron Mn particles. Indeed, Bishop and Fleisher (1987) report a 40% lower Mn content of QMA filter samples when only 25% of the intended water volume was sampled, but found no difference in Ca content, which was dominated by 1-5 µm sized coccoliths. There was no systematic difference in 1-51 µm Ca concentrations between the main and auxiliary flow paths at SAFe (not shown), consistent with these results. This comparison demonstrates that we can in principle compare the concentration profiles of the suspended size fraction across multiple casts at SAFe, as well as between the main 293 mm and auxiliary 142 mm flow paths, with the caveats associated with Mn.

In comparison to the QMA filter suite, the cast-to-cast variability in concentration profiles collected on 0.45 µm Supor filters on the auxiliary flow path on cast M09 and the main flow path on cast M10 is higher for all elements (Fig. 6B). The agreement between the two casts is relatively good for Cd, although the shapes of the profiles are less smooth than from the QMA filters (Fig. 6A). Particulate phosphorus collected during cast M9 is ~30% lower than that collected during cast M10, despite beam attenuation profiles that show slightly higher particle concentrations in the upper 150 m during cast M9 (Fig. 4). The agreement is worst for Mn and Ba below 200 m, with concentrations ranging by factors up to 3-4 between the two casts. The discrepancies in Mn concentrations cannot be explained simply by loading differences between the main and auxiliary filter. While there is some hydrographic variability between casts M09 and M10 in the upper 200 m that may explain some of the cast-to-cast variation in the euphotic zone, there is little change in hydrography below 250 m (Figs. 3 and 4). Thus, the large variability between casts demonstrates the difficulty of obtaining reproducible results from 0.45 µm Supor filters. These findings indicate a very nonuniform distribution of particles on the 0.45 µm Supor membrane filters (Fig. 7) and reflect the error due to the unintended subsampling of an area with lower particle loading.

Finally, we plot the concentration profiles for the four different types of filters used at the SAFe station together to compare their relative efficiencies of particle collection. One would expect the smaller pore-size filters to collect more material. Particulate Cd and P concentrations in the euphotic zone are indeed generally higher when collected on either 0.45 µm or 0.8 µm Supor filter compared with QMA filters (as also seen in Fig. 6) and higher still when collected on 0.45 µm MF filters (Fig. 8). In contrast, particulate Mn and Ba concentrations below 200 m are significantly lower on MF and Supor compared with QMA filters (Fig. 6B), despite the larger nominal pore size of the QMA filters. We further found that concentrations from the 0.45 µm Supor filters were not necessarily higher than those collected on 0.8 µm Supor filters. The deep Mn and Ba concentrations from the 0.8 µm Supor filter are higher than those collected on either of the 0.45 µm filters despite having a larger nominal pore size.

In sum, these profiles suggest that the 0.45 µm pore size filters have problems. While the Mn and Ba profiles collected on 0.8 µm Supor filters are still low compared with the QMA profiles, the discrepancy is much smaller, suggesting that the collection problems are not as severe.

As we discuss below in the imaging section, we believe that the filtration characteristics of both types of 0.45 µm filters make them an unsuitable choice for in-situ filtration.

Effect of filter type on < 51 µm particle distribution

Original photographic images of dried micron and submicron filters show the increasingly poor distribution of particles as one switches from QMA to 0.8 µm Supor to 0.45 µm Supor filters on either the 293 mm (Fig. 7A) or 142 mm filter holders (Appendix: Fig. S4) with increasing depth below 200 m. The particle distribution on 142 mm 0.45 µm MF filters was no better than on 0.45 µm Supor filters (Appendix: Fig. S4). The heterogeneity in particle distribution is increasingly large in deep samples (Fig. 7B-D) and as one goes from QMA to 0.8 and 0.45 µm Supor filters. For example, gray scale count (standard deviation and percent relative standard deviation in parentheses) differences relative to an unused blank filter reference along transects shown in the figure were 57 (SD = 2.6; RSD = 4.6%), 19 (SD = 3.4, RSD = 17%), and 9 (SD = 4.1,RSD = 45%) for QMA, 0.8 µm Supor and 0.45 µm Supor filters from 845 m, respectively. Since the particulate concentrations are determined on leaches of subsamples that typically represent 2.5% of the main 293 mm filter or 10% of the auxiliary 142 mm filter, a heterogeneous particle distribution can lead to severe biases and is likely the one major reason for the large discrepancies in particulate Mn and Ba concentrations below 200 m seen between filter types (Fig. 6B). The cause of the poor particle distribution at depth is not known, but since heterogeneity increases with depth, we believe that the Supor and MF material is distorted by pressure. Centimeter-wide patterns in surface reflectivity were readily observable in unused 293 and 142 mm Supor filters under side illumination.

We further found some millimeter-sized particle aggregates on the 0.45- 51 µm sample from 845 m on both main and auxiliary filters. These appear to result from the aggregation of particles resuspended from the filter into the partially air-filled headspace immediately above the filter as residual water is being removed from the filter holder by vacuum during and after pump removal from the wire. We have not investigated other brands of polyethersulfone or mixed cellulose/acetate membrane filters. The aggregation of particles was not observed in QMA samples.

Effect of pairing filters on sampled small particle population

Because QMA and Supor filters both work as depth filters, deploying them as pairs increases the effective depth, and thus efficiency, of particle capture, reducing the nominal pore size (See e.g., Bishop and Edmond 1976). The profiles from paired top and bottom QMA (Fig. 5) and 0.8 µm Supor filters (Fig. 8) show that particles captured on the bottom filter can con-

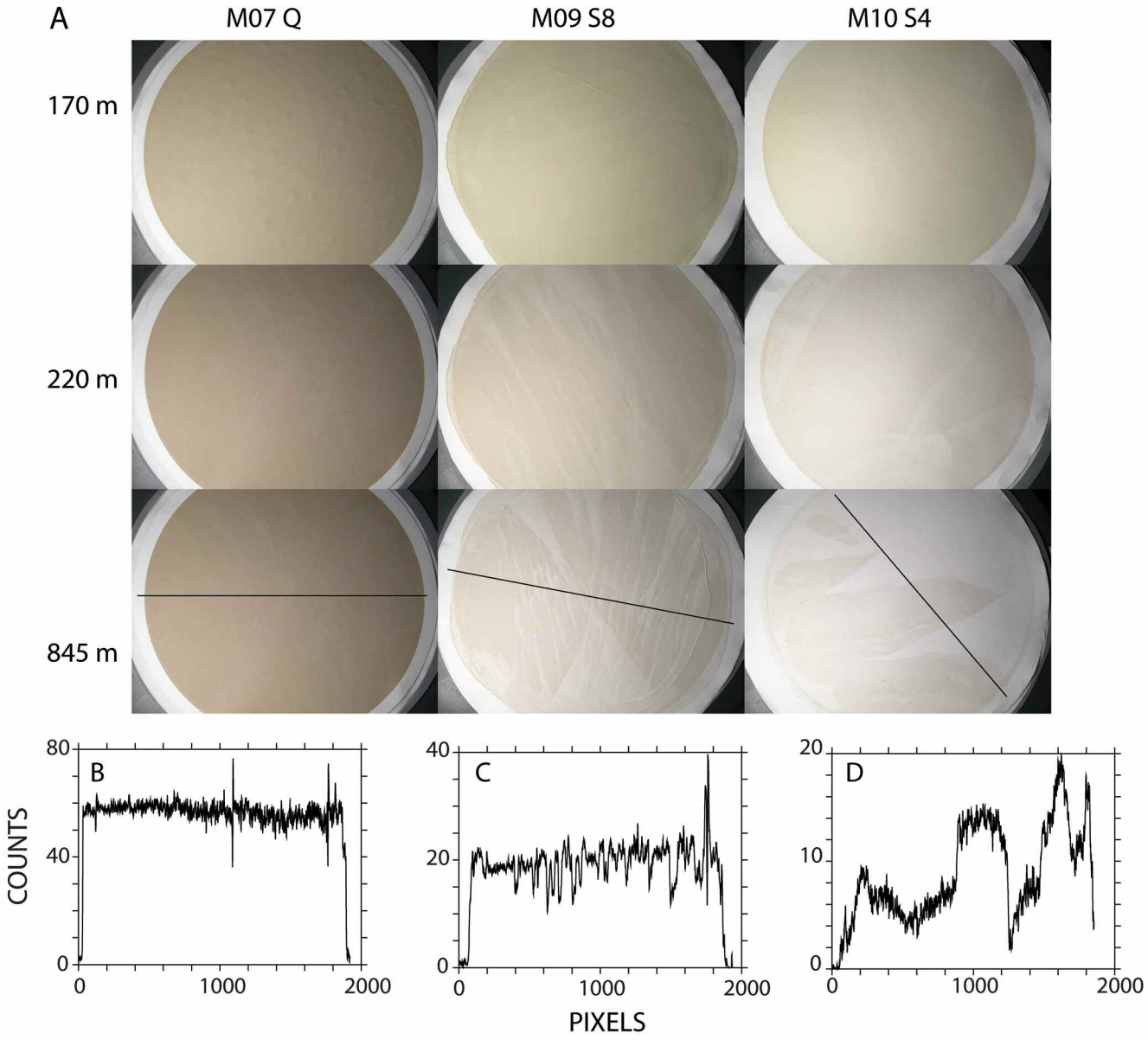

Fig. 7. (A) At-sea photographic images of dried QMA, 0.8 µm and 0.45 µm Supor filters from the main filter samples from casts M07, M09, and M10 at 170, 220, and 845 m. (B), (C), and (D) are profiles of the gray scale counts (blank – sample) along the depicted transects through 845 m QMA, S8 and S4 filters, respectively. Supor filters become increasingly streaky and inhomogeneous in distribution deeper than 200 m. We also found millimeter size aggregates in areas of the 0.45 µm Supor filter from 845 m suggesting resuspension and reaggregation of collected sample.

tribute significantly to the total profile, especially for biogenic elements in the upper 200 m, such as P and Cd, that may be associated with sub-micron picoplankton or heterotrophic bacteria. We compare the concentration profiles derived from the sum of top and bottom QMA and 0.8 µm Supor filters to those from single filters of 0.45 µm pore-size in the upper 200 m, where filter sample homogeneity is comparable with QMA samples. The observed hydrographic variability in the upper 200 m over the course of these three casts slightly complicates the interpretation of this comparison, since the transmissometer-derived particle concentrations drop from casts M08 through M10 (Figs. 4). However, the filter pore sizes in this depth range behave as expected over the course of the three casts, with the two 0.45 µm filter types (S4 and MF) deployed during casts M09 and M10 collecting more material than the 0.8 µm Supor filter deployed during cast M08.

Concentration profiles derived from the sum of the top and bottom QMA filters are similar to those from a single 0.8 µm Supor filter (Fig. 8), suggesting that paired QMA filters sample a population similar to a single 0.8 µm Supor—consistent with Coulter Counter studies on the behavior of glass fiber filters reported by Bishop and Edmond (1976). Concentrations

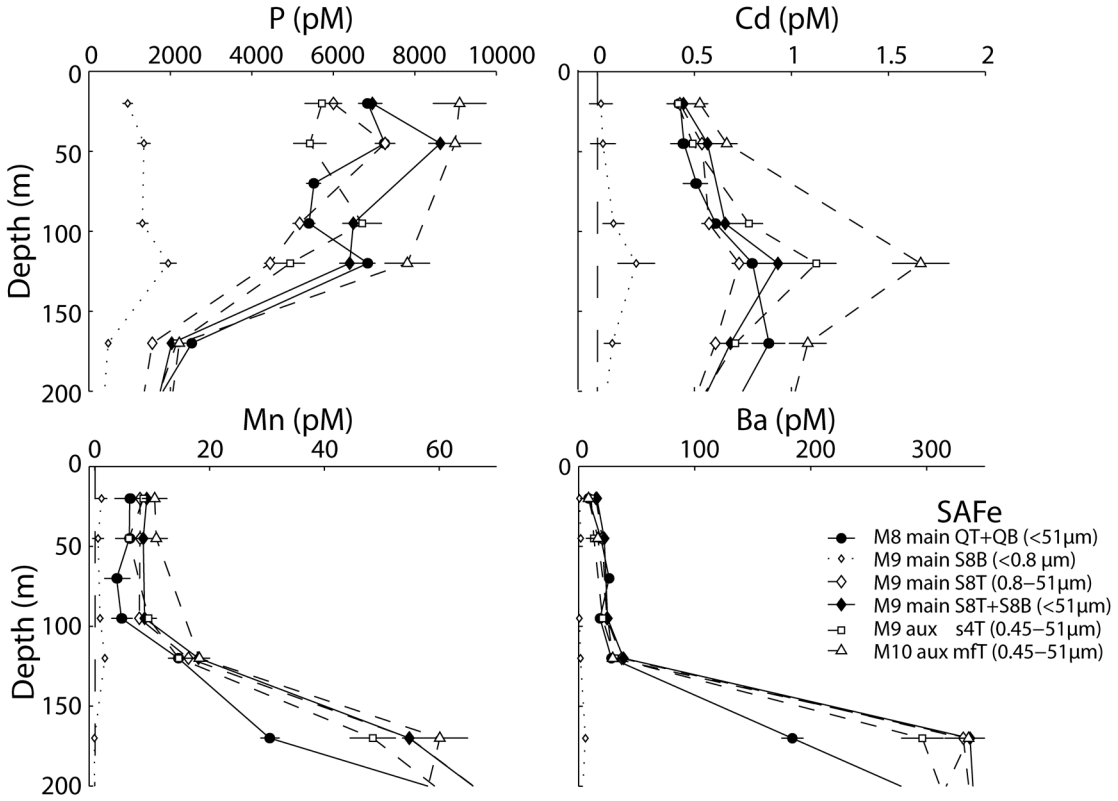

Fig. 8. Concentration profiles for P, Cd, Mn, and Ba in the upper 200 m at for MULVFS casts M08, M09, and M10 at SAFe. Profiles compare the sum of top and bottom QMA (QT + QB); the bottom, top 0.8 µm Supor, and their sum (S8B, S8T, S8T + S8B); the top 0.45 µm Supor; and the top 0.45 µm MF. Error bars are as in Fig. 6. In this depth range, the filter pore-sizes behave as expected, with the 0.45 µm filters (open squares and triangles) collecting more than the 0.8 µm Supor (open diamonds). The sum of top and bottom QMA (filled circles) is similar to the top 0.8 µm Supor (large open diamond), suggesting that paired QMA filters sample a population similar to a single 0.8 µm Supor. The sum of top and bottom 0.8 µm Supor (filled diamonds) is intermediate between that for 0.45 µm Supor (open squares) and MF (open triangles) filters.

derived from the sum of the top and bottom 0.8 µm Supor filters are higher than those from the paired QMA filters, and generally fall in between those from 0.45 µm Supor and 0.45 µm MF filters (Fig. 11), suggesting that paired 0.8 µm Supor filters collect a particle population similar to a 0.45 µm filter. While deploying paired 0.8 µm Supor filters may not exactly sample a > 0.45 µm particle population, its better particle distribution and loading characteristics compared with the 0.45 µm filters make them a better choice for in-situ pumping.

Filter holder experiments on IC1: particle loss from > 51 µm size fraction

During IC1, we compared the particle collection characteristics of 142 mm filter holder types B-D (Table 3) loaded on the auxiliary flow path to those of the MULVFS filter holder (type A1) on the main flow path. During each cast, McLane-style (type B) holders were deployed on six pumps, and variants of filter holder types C and D were loaded on the other six pumps. The positions of the filter holder types in the water column were changed each cast. The first two casts at BATS (M01 and M02) were meant primarily for filter holder intercomparison experiments, and the standard QMA filter suite was loaded in all filter holders. Mn-coated cartridges for radionuclide adsorption were installed downstream of the auxiliary holders on cast M02. During cast M03, a mix of submicron filter types was loaded onto the auxiliary flow paths, slightly complicating the interpretation of the auxiliary > 51 µm prefilter results because of the additional effect of varying face velocities (cf. Figs. 16, 17), but providing further combinations of filter holder types throughout the water column.

Greater than 51 µm Mn levels were at detection limits in the upper 100 m; in deeper samples, there was no systematic gain or loss of > 51 µm Mn in the 142 mm filter holders at M01, M02, or M03 (Figs. 9-11). We are unable to explain why the 142 mm holders (B1, B2) on cast M02 at 200 m and 250 m collected more > 51 µm Mn than the main MULVFS holder. Concentrations of > 51 µm Ba in the 142 mm holders were within error in casts M01 and M02, but were a factor of two lower in shallow B2 and C1 holders at M03, despite generally lower auxiliary face velocities due to smaller pore-size submicron filters. Most variants of the 142 mm filter holders tested during IC1 showed considerably lower concentrations of > 51 µm P and Sr (up to factors of 4 to 8, respectively at M03) compared with the main 293 mm MULVFS filter holders in all three casts, especially in the upper 200 m (Figs. 9-11).

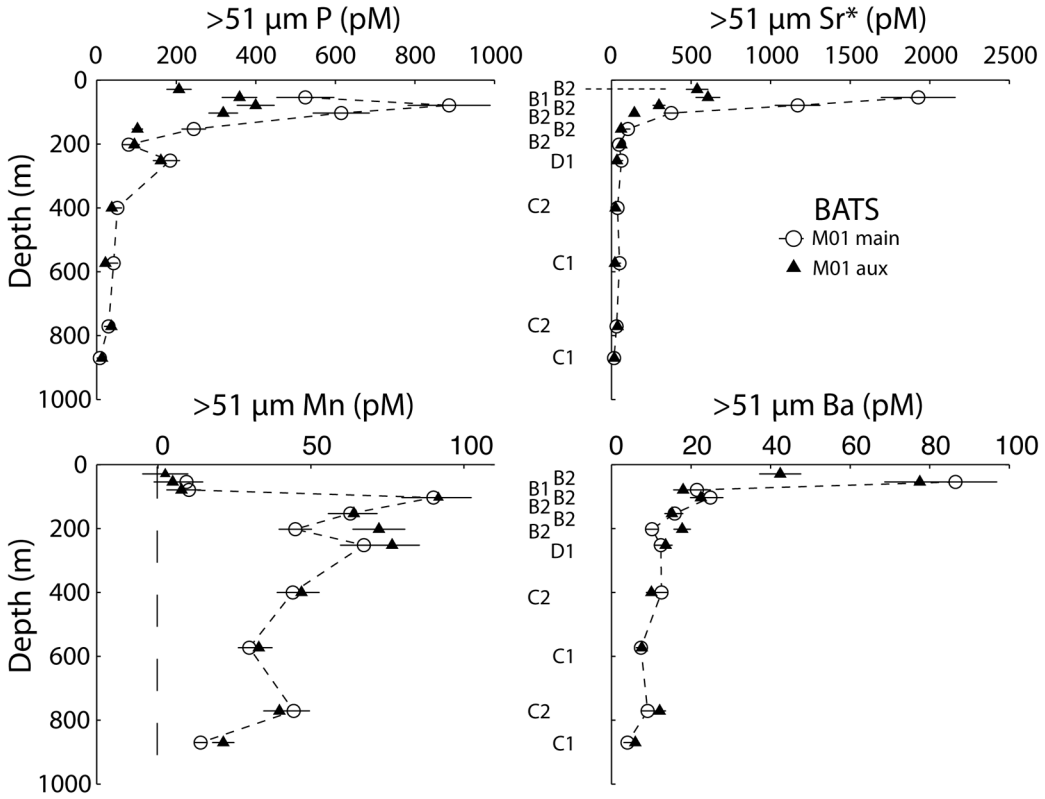

Fig. 9. Greater than 51 µm P, Sr*, Mn, and Ba from MULVFS cast M01 at the Bermuda Atlantic Time Series station from the main versus auxiliary flow paths (solid triangles). Error bars are as in Fig. 6. Letters A1 through D1 placed in the center of the figure denote the 142 mm auxiliary filter holder type used for sampling.

This suggests a preferential loss of biogenic material—fresh aggregates, live phytoplankton, and Sr-containing acanthar-ians—from the filter holders that we tested. Since particulate phosphorus is the primary indicator of biogenic material from ICP-MS methods, its accurate collection is crucial for the interpretation of particulate trace elements and isotopes.

The exception to the rule of systematic under-collection of > 51 µm P by 142 mm filter holders was the significantly higher concentrations at 80 m and 105 m during cast M02 (Fig. 11). The auxiliary flow paths on these pumps were loaded with D-type filter holders, which both had a central elbow-shaped intake protruding from a solid top plate. We observed numerous zooplankton collected on the 51 µm prefilter of these two holders, which may explain the anomaly in P but not in the other elements. The filter holders with large intake areas (holder types A, B, C) have a slow enough intake velocity that zooplankton can presumably sense the flow and escape (see Bishop and Wood 2008 for additional discussion). The cross-sectional areas of the elbow-intakes for the D-type filter holders are smaller and lead to a higher intake velocity, likely preventing zooplankton from swimming away. Indeed, holder D2, whose intake orifice area is 30 times smaller than that of holder D1, had an even higher anomaly in > 51 µm P (factor of 3.5) compared with the adjacent 293 mm MULVFS holder than holder D1 (factor of 1.5). The high number is also due to the fact that the center one third of the area of the D2 filter was almost clean of particles, and it is likely that subsampling took place in an area of the filter where particles were present. Holder type D1 was also deployed on cast M01 at 252 m without enhancement of > 51 µm P. We interpret this to reflect lower swimming zooplankton abundances at this depth and time of sampling compared with the shallower placement of this holder at 80 m on cast M02.

The loss of > 51 µm P or Sr* were not alleviated by the extra baffle stage in holder C2 compared with C1 during cast M3 (Fig. 11), nor by the taller plastic baffle in holder B5 during cast M05 (not shown). Likewise, mixing and matching the plastic and metal baffles and prefilter support plates (holders B3, B4) did not seem to make a difference. This suggests that simple fixes to the existing filter holders were not going to solve the problem of loss of large biogenic particles.

Filter holder experiments on IC2: new mini-MULVFS 142 mm holder

Because all 142 mm filter holders that we tested in IC1 had significant problems in collecting biogenic material even in most benign oceanographic conditions (no current, no waves, no swell, no wind) of IC1, we opted to design a new 142 mm filter holder based on the 293 mm main MULVFS filter holder. The "mini-MULVFS" holder (holder type A2—Fig. 2) adopts the 3-baffle system used by the main MULVFS holder to ensure

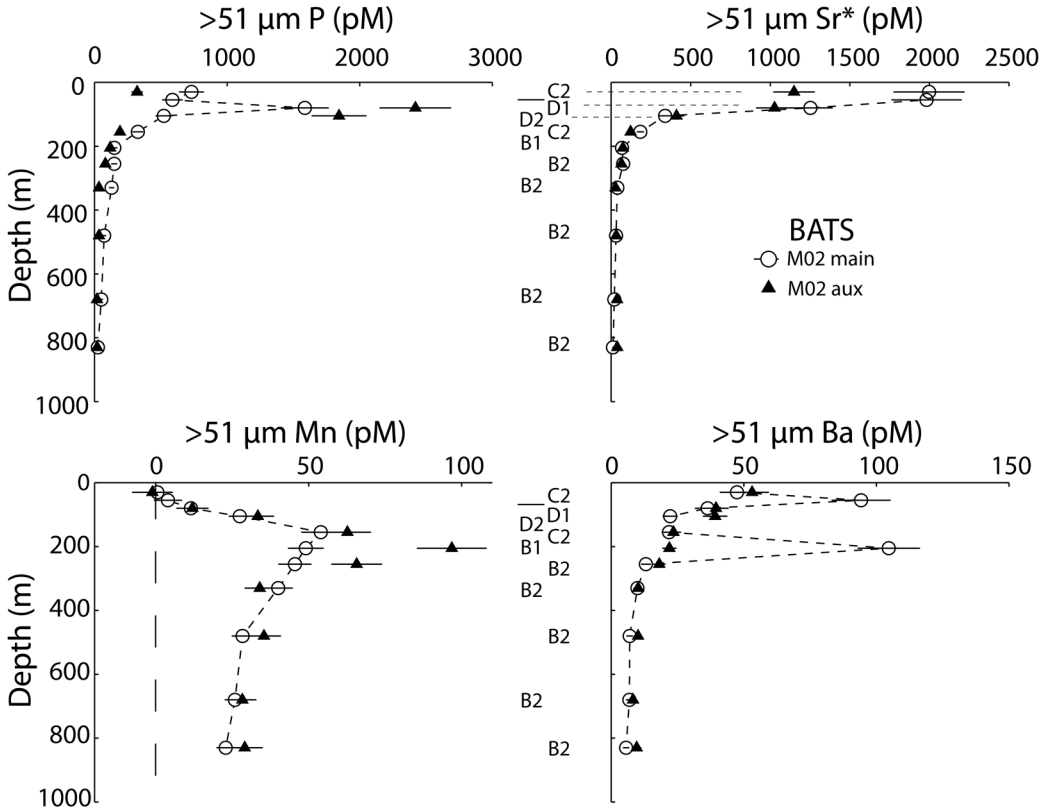

Fig. 10. Greater than 51 µm P, Sr*, Mn, and Ba from MULVFS cast M02 at BATS. Symbols, error bars, and annotations as in Fig. 9. The auxiliary sample from 55 m recorded zero flow and is not plotted. The 205 m main Ba value is anomalous.

even particle distribution and large particle retention. During IC2, we restricted our 142 mm filter holder experiments to just the newly designed mini-MULVFS holder (A2) and the all-plastic McLane style holder for trace metal applications (B2). Similar to IC1, the first two MULVFS casts (casts M07 and M08) at the oligotrophic station (SAFe) and the first cast at the mesotrophic Santa Barbara Basin (SBB) station were devoted to filter holder comparisons, and all holders were loaded with the standard QMA suite of filters. At SAFe, five filter holders of type B2 were deployed in the upper 150 m in the first cast (M07), and below 150 m in the second cast (M08), with the remaining pumps populated by holder type A2. At SBB, holder type A2 was deployed exclusively on the auxiliary flow path of all pumps.

We replicated the loss of > 51 µm P and Sr* from the McLane holders (type B2) during IC2 (Fig. 12, open triangles), with the most prominent loss found in the upper 150 m (Fig. 12A), as during IC1. Holder type B2 further showed loss of > 51 µm Mn in the upper 150 m (Fig. 12A), but over collection of Mn below 150 m (Fig. 12B). In contrast, the new mini-MULVFS holder reproduced the main 293 mm holder results for all four elements at SAFe in both the upper and lower water column, solving the upper water column particle loss issues evidenced by > 51 µm P and Sr*, and more faithfully reproducing the > 51 µm Mn profile throughout the water column (Fig. 12). As noted earlier, both 142 mm holder types A2 and B2 performed equally well for the 1-51 µm suspended size fraction (Fig. 6A), confirming that the loss of particles observed during IC1 was restricted to the > 51 µm sinking size fraction.

Samples from cast M11 at SBB also showed good agreement of > 51 µm P, Sr*, and Ba concentrations between the main-MULVFS (A1) and mini-MULVFS (A2) filter holders (Fig. 13), demonstrating that the mini-MULVFS filter holders perform well in both oligotrophic and mesotrophic environments. The > 51 µm Mn concentrations at SBB are consistently 10% to 20% higher in the mini-MULVFS holders. This is unlikely to be due to flow-dependent effects as the average flow velocities at the face of the filters were quite similar. We noted that significant material (which must have been close to the 50 µm mesh size) was wicked onto to the sample rinsing stand during the process of collection of fresh subsamples from MULVFS (A1) prefilters.

We further tested the mini-MULVFS (A2) and McLane (B2) holders side by side in a McLane pump "rosette" deployed at SAFe and in the Santa Barbara Basin. This permitted the simultaneous comparison of the two 142 mm filter holder types, which was not possible on the MULVFS. We loaded four of each type of 142 mm filter holder (A2 and B2) on eight McLane pumps around the 8-pump rosette, four of these samples were available for our analysis. We found that the distri-

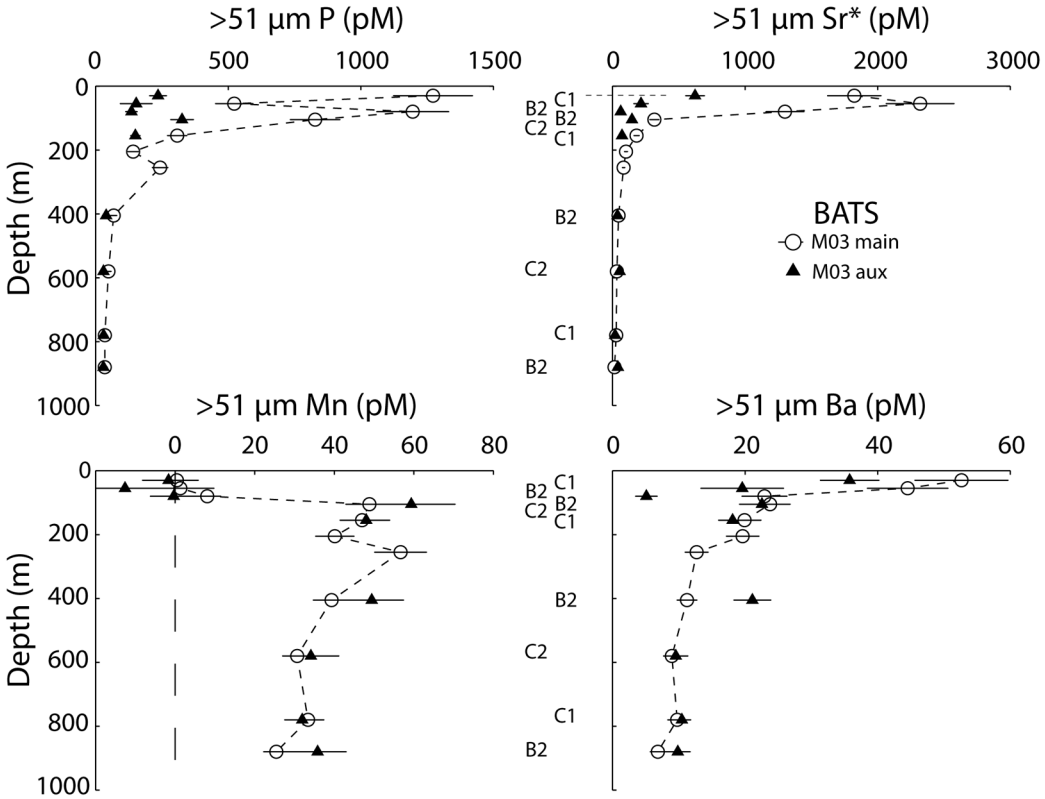

Fig. 11. Greater than 51 µm P, Sr*, Mn, and Ba from MULVFS cast M03 at BATS. Symbols, error bars, and annotations as in Fig. 9. 150 µm filters were loaded in samples from 205 and 255 m by accident. Aux. data are not plotted.

bution of > 51 µm particles on the prefilters from the A2 holder was far superior to the distribution from the McLane (B2) prefilters (Fig. 14). The figure shows an image of a 150 µm filter (mounted in a type B2 holder at rosette position 7), which was accidentally mounted as a prefilter during the SAFe deployment. The sample is included because it shows complete loss of large millimeter-sized particles compared with those collected using holder type A2.

Effect of (sub)-micron filter type on volume throughput, flow rate, and particle loading

The MULVFS uses centrifugal pumps, which means that the pressure drop across the filter rises only a factor of two to a maximum of 0.8 atm as filters become loaded to capacity and flow goes to zero (Bishop et al. 1985). The micron or submicron filter collecting the < 51 µm particles slows down the volume flow rate and the resulting face velocity felt at the prefilter surface is thus lower. Most pressure differential develops across the filter collecting < 51 µm particles. Compared with paired QMA filters, paired 0.8 µm Supor filters (S8^2) or a single 0.45 µm Supor filter (S4) allow only ~40% of the volume of seawater to be filtered over the same pumping time. The smallest pore size 0.2 µm Supor filters allow only ~10% of the QMA flow volume (Table 1). In absolute terms, the volume of water filtered through main QMA filters at BATS ranged from near surface values of ~2500 L in surface waters to 14,000 L at 600 m. Auxiliary samples filtered ~600 L in surface waters to ~2000 L deeper. Side-arm samples ranged from ~10 L in surface waters to ~60 L in deeper waters.

When we divide flow rate by filter area, it is possible to calculate a water flow velocity to the surface of the filters. We call this 'face' velocity. The range is from < 0.15 cm/s to ~1.6 cm s^{-1} in the main filter holder, from ~0.1 to ~1.1 cm s^{-1} in the 142 mm holders, and from 0.04 to 0.22 cm s^{-1} in the 47 mm side-arm holders (Figs. 15, 16). For comparison, a McLane pump operating at the typically used flowrate of 6 L min^{-1} through a McLane 142 mm filter holder with active area of 132.7 cm^2 would have a face velocity of 0.75 cm s^{-1}. The maximum McLane flowrate of 8 L min^{-1} would yield 1.0 cm s^{-1} face velocity. Relative particle loading of filters would scale exactly to these numbers.

Effect of flow rate on > 51 µm particle concentrations

The actual flow velocity through the prefilter depends on both the open area of the filter mesh and on the open area of the prefilter support plate. For holders with "egg crate" or square grid prefilter supports (types A, C, and D; Table 3), the true face velocity through the polyester prefilter is determined by its 33% open area because the open area of the filter support immediately downstream is more than 95%. The flow velocity felt at holes of the prefilter is therefore ~3 times higher than that calculated from volume flowrate alone. On

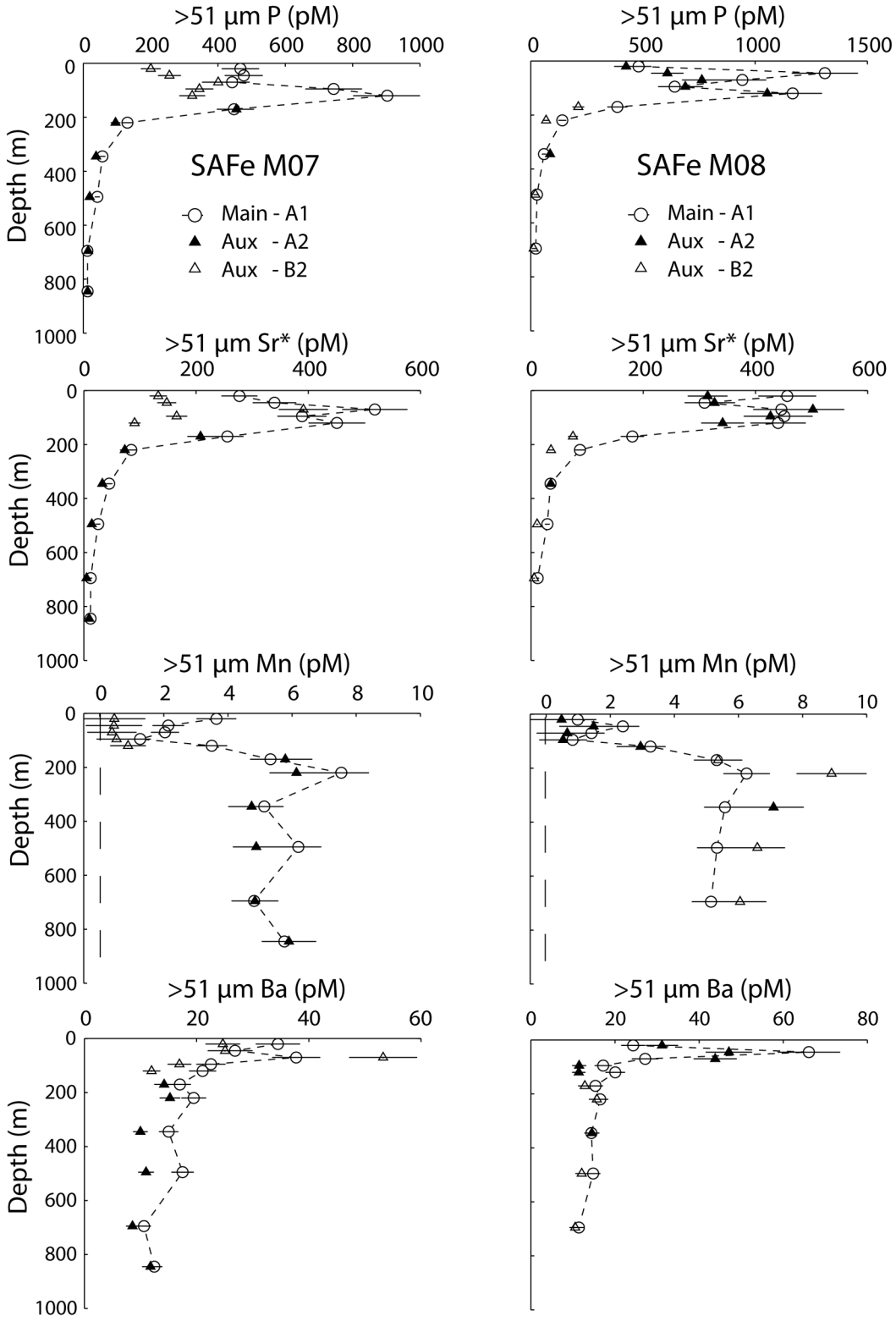

Fig. 12. (Left) Comparison of large particle concentration profiles at SAFe from MULVFS main (type A1) and auxiliary (holder type B2 used shallower than 180 m, A2 used deeper) samples collected during MULVFS cast M07. Error bars are as in Fig. 9. Data reproduce findings from the C1 expedition that shows enhanced loss of most elements from holder type B2 in waters shallower than 150 m. (Right) Similar data for Cast M08. A2 holders were deployed shallower than 180 m, whereas B2 holders were used for deeper samples. Results show good agreement with main prefilter samples for all A2 holders.

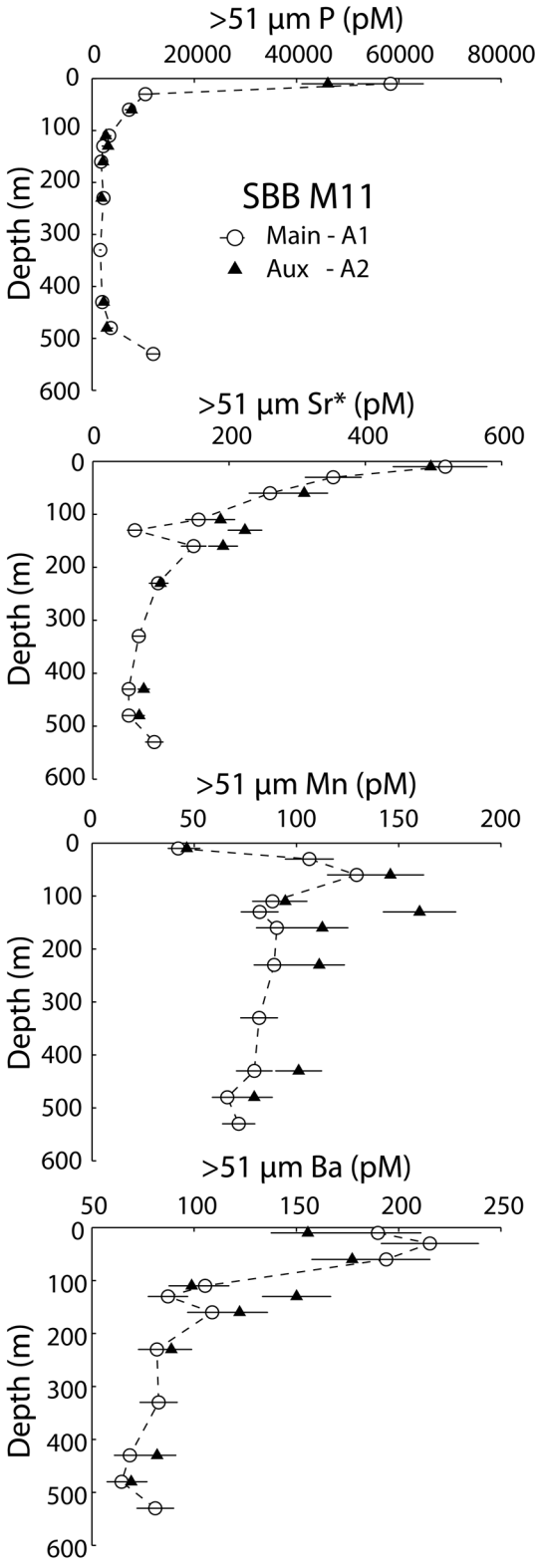

Fig. 13. Comparison of large particle concentration profiles in the Santa Barbara Basin from MULVFS main (type A1, open circles) and auxiliary (type A2) samples collected during MULVFS cast M11. Error bars are as in Fig. 9. Only type A2 filter holders were used during sampling.

the other hand, the plastic-variant of McLane filter holders (types B2, B4, B5; Table 3) has a perforated prefilter support plate with only 40% open area. The flow velocity felt through the holes of the prefilter in these types is higher by another factor of 2.5 (7.5 times faster). Thus the actual flow velocity at the prefilter holes for MULVFS main samples is up to 4.8 cm s^{-1} whereas that for auxiliary B2 holders on MULVFS is as high as 8.3 cm s^{-1}. Individual McLane pumps (typically running at 6L/min) with B2 holders have velocities of 5.6 cm s^{-1}.

During IC1, we used photography to derive volume and area normalized green optical density (OD) profiles of > 51 µm particles from main and auxiliary samples for MULVFS casts at BATS. Data showed good agreement (Fig. 15) among main prefilter samples for casts M01 through M03 but significantly higher OD values were found in deep water from cast M04 at depths where either paired 0.8 µm or single 0.45 µm Supor filters were used. QMA-backed samples from M04 agreed closely with the other casts. The flow velocities of water through the main QMA backed prefilters on casts M1, M2, and M3 were approximately 2.5 times higher than through Supor-backed prefilters at M04 because Supor filters restricted the flow. Fig. 15 also shows that almost all of the data from auxiliary filters fell at or below the optical density profile trend established from main samples from M01 through M03 and significantly below the trend established by main M04 Supor-backed prefilters. Given that the main MULVFS filter holders are believed not to lose particles post collection, the main filter results suggest some effect of flow velocity on the efficiency of > 51 µm particle collection.

During IC2, we used the "filter type" deployments to systematically test the effect of water flow velocity on the chemical composition of the > 51 µm size fraction. Fig. 17 shows face velocity profiles for main and auxiliary samples during IC2. We focus on intercomparison of profile results at depths 495, 695, and 845 m at SAFe where hydrographic variability was shown above to be small. We further restricted comparisons to filter holders A1 and A2, main-MULVFS and mini-MULVFS (Fig. 1 and Table 4), since other designs were shown to be subject to washout or other biases. In the cases of Mn, Ba, and Ca, concentrations decrease no more than 50% between flowrates of 0.1 cm s^{-1} and 1.6 cm s^{-1}. The curious finding is that P shows no flow rate dependence. Ca, Mn, and Ba in the > 51 µm size fraction are typically aggregations of much smaller (micron-scale) particles of these elements ($CaCO_3$ coccoliths, Mn oxyhydroxides, and barite). We hypothesize that the organic fraction containing P is more cohesive and thus not subject to flow induced aggregate erosion.

Bishop (1982) investigated flow velocity/capture efficiency of large particles over a much higher range of flow velocities greater than used in MULVFS and concluded that greater than 90% of visible (>1 mm) large aggregates were retained at flow rates 1.5 times faster than used by MULVFS. Here, we compare aggregate particle size distributions down to 150 µm from main and auxiliary samples collected at a

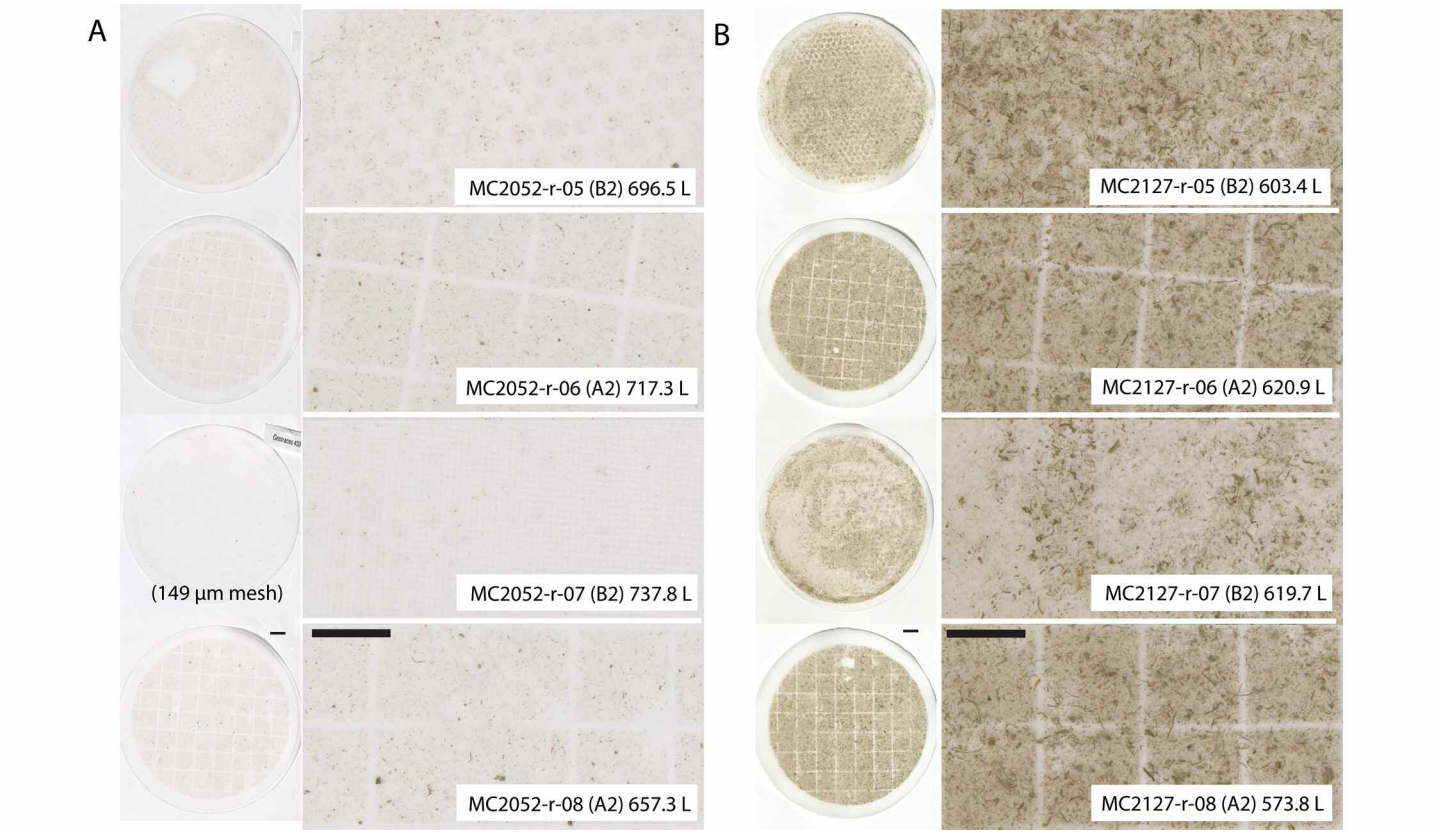

Fig. 14. (Left) Photographs of > 51 µm samples collected using McLane "TM" (type B2) and "mini-MULVFS" (type A2) holders during GEOTRACES IC2 McLane rosette cast 2052 at the SAFe station. All samples collected simultaneously at a depth of 120 m. Images are of whole 142 mm diameter filters obtained under uniform lighting and are shown magnified 3.5_ on the right. Scale bars denote 1 cm. Sample MC2052-r-07 was collected using two layers of 150 µm mesh rather than the standard 51 µm/150 µm arrangement. Note the general absence of large particles in this sample and MC2052-r-05 compared to Mini MULVFS samples. (Right) Photographs of > 51 µm filter samples collected using McLane "TM" (type B2) and "mini-MULVFS" (type A2) holders during GEOTRACES IC2 McLane rosette cast 2127 in the Santa Barbara Basin. All samples were collected simultaneously at a depth of 110 m.

depth of 345 m during MULVFS casts M08 (face velocity: main = 1.45 cm s^{-1}, aux = 0.99 cm s^{-1}) and M09 (main = 1.53 cm s^{-1}, aux = 0.53 cm s^{-1}) to investigate flow effects (Fig. 18). These particular samples were chosen because they had relatively elevated abundances of large aggregate particles. As noted above, they were also collected using filter holders A1 and A2, which have been shown to have almost identical performance. We observed little obvious difference in aggregate size distribution in cast M08 samples suggesting that face velocities of 1 and 1.5 cm s^{-1} yield similar results. Comparisons of particle size distributions at M09 suggested that there may be about a 0.1 log unit (or 25%) relative increase in aggregate abundances across the large particle size spectrum at a filtration face velocity of 0.5 cm s^{-1} versus the 1.5 cm s^{-1} typically used during standard MULVFS sampling. Taken together, the optical particle concentration proxy profiles, particle size distribution data, and chemical data for the deep > 51 µm samples suggest that in situ filtration flow bias effects can lead to at most factor of two differences in particles sampled from the upper kilometer. The biases appear low for organic bound species.

MULVFS, McLane Rosette, McLane Profile comparison

Fig. 19 shows optical density profile data obtained in the Santa Barbara Basin during casts M11 (event 2110) and M12 (event 2125) with data from samples collected using the McLane rosette system at 110 m (event 2127, samples shown in Fig. 14) and with samples collected using wire-deployed McLane pumps (event 2129). Type A1 and A2 holders were exclusively used during MULVFS casts, a mix of type A2 and B2 holders was used during the rosette cast as previously noted, and type B2 holders were used exclusively during the McLane profile. Three of four rosette samples fall quite close to the trend defined by MULVFS profiles (rosette position 7 low). The data shallower than 300 m from the McLane profile fall at least a factor of two low.

Discussion

We found that all filter holder types tested yielded comparable samples of the small particulate fraction when filters of the same pore size were used. We found that paired QMA filters collect similar quantities of particles as captured on a single 0.8 µm Supor filter; furthermore, paired 0.8 µm Supor fil-

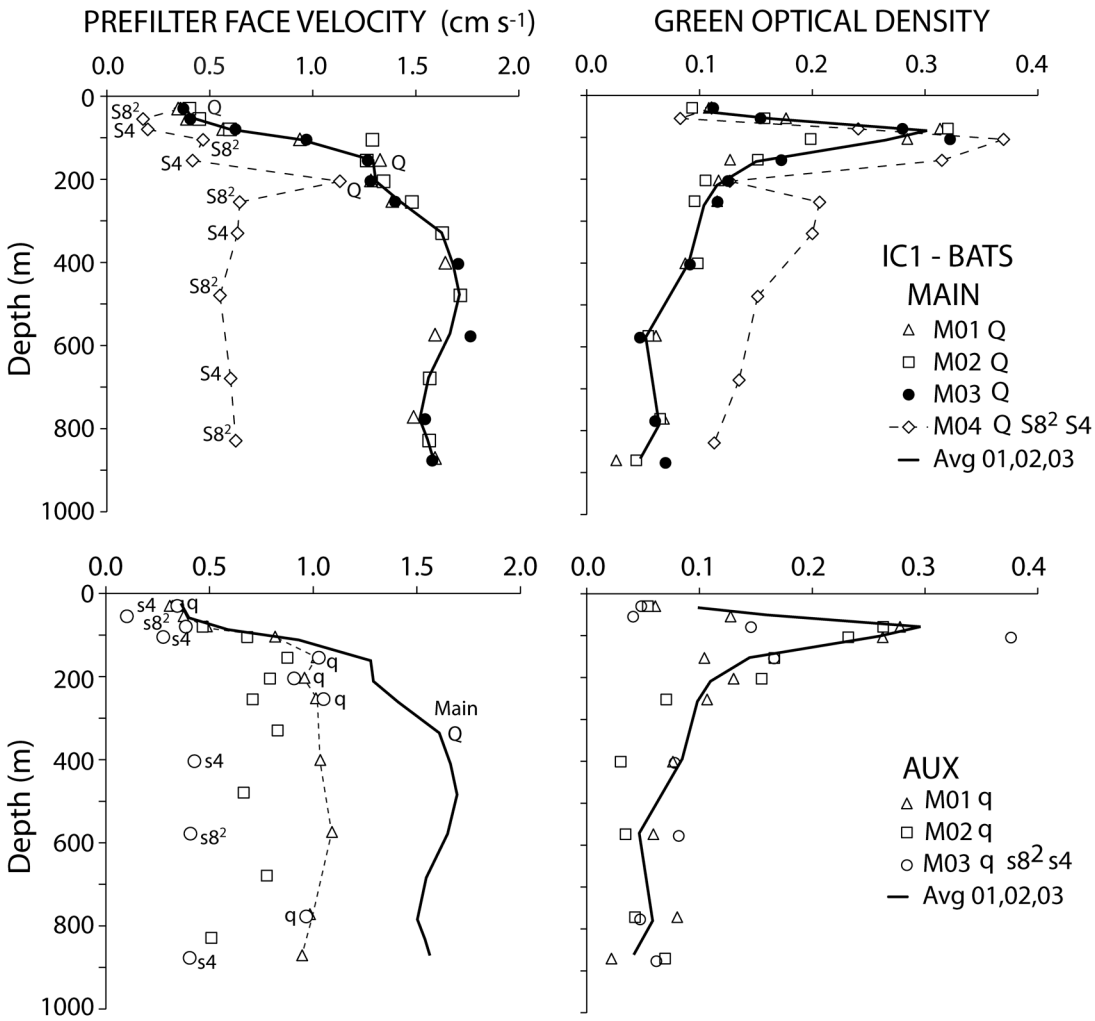

Fig. 15. Plots showing prefilter face velocity, and the volume and area scaled green optical density for MULVFS profiles M01, M02, M03, and M04 at BATS during IC1. Top panels denote Main channel data. Lower panels denote auxiliary channel data. Variations of prefilter face velocity were a result of different filter types (QMA, Supor 0.8 µm, Supor 0.45 µm) used to collect the small particle size fraction. M04 Samples at 30 m and 205 m were collected using QMA filters and agree closely with data from the other casts. Solid lines in all figures represent the average of main flow channel results from casts M01, M02, and M03. The auxiliary sample OD data frequently fall below the optical density trend from main filter samples (M01, M02, and M03) and indicates large particle loss from most filter types tested. The higher OD values in main samples for cast M04 show that samples taken with lower prefilter face velocity yield higher values.

ters yield particle abundances close to that of a single 0.45 µm Supor or Millipore (MF) filter. We showed that particle distributions at 800 m were most even across QMA filters (<4% RSD), followed by 0.8 µm Supor (17% RSD) and 0.45 µm Supor Filters (~45% RSD). Consequently, paired 0.8 µm Supor filters are better than a single 0.45 µm filter for applications requiring both subsampling and total sample digestion.

In a comparison with the three-baffle MULVFS filter holder, we found that all single and double baffle filter holder types lose large particles, especially in the upper 150 m. This finding is consistent with differences reported by Gardner et al. (2003), Liu et al. (2005), and Liu et al. (2009). The loss of the large particle fraction described above is likely to be underestimated compared with real ocean conditions because both IC experiments took place in conditions of calm winds and absent of swell. Reinforcing this finding is the observation that type B2 filter holders deployed on the McLane rosette appeared to be less subject to particle loss than when they were attached to McLane pumps attached to a wire. This suggests that wire angle or other wire/pump motion dynamic enhances the turbulent regime in the side slotted holders. We have clearly demonstrated that the mini-MULVFS holder (A2) solves the problem of > 51 µm particle loss that was apparent in the McLane holders (B2) in both the upper and lower water column (Figs. 12-13).

The loss of large particles that is particularly evident on the McLane type holders (type B) is likely due to a number of factors. The perforated polypropylene disc used as a prefilter sup-

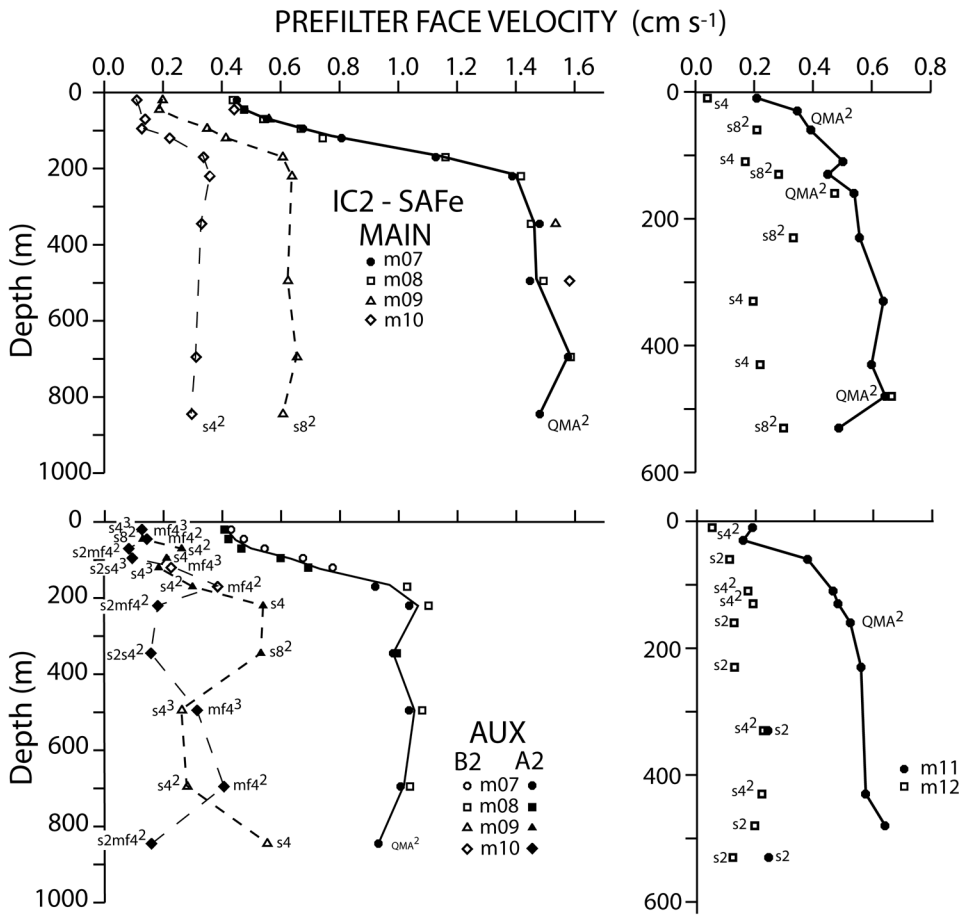

Fig. 16. Average prefilter face velocity through filters during MULVFS casts M07-M10 at SAFe and casts M11 and M12 in the Santa Barbara Basin during IC2. Top and bottom panels denote data for main and auxiliary flow channels, respectively. Data points are annotated with filter type used to collect small particles. Actual flows through the holes in the 51 µm mesh of the prefilter are 3 times higher due to the mesh having 33% open area.

port in the all-plastic version of the McLane holder (B2) resulted in a poorer > 51 µm particle distribution compared with the stainless steel mesh prefilter support of the standard McLane holder (B1), but both experienced similar loss compared with MULVFS (Figs. 9, 10). Since the distribution of particles is also worse when the perforated polypropylene disc is used as a prefilter support, this may exacerbate particle loss. We noted that the polypropylene disc often does not lie completely flat, and that the polypropylene material floats in water. While small tabs on the stage above it prevent the disc from floating away, the buoyancy may nonetheless promote particle redistribution. Second, the percent open area of the perforated disc is only 40%. This has the effect of increasing the apparent flow velocity experienced by the particles as they impact against the prefilter surface by a factor of 2.5. As we showed above, an increase in face velocity can lead to a decrease in the concentration of > 51 µm particles collected by MULVFS. Some samples collected using the McLane type B holders were filtered at a rate effectively twice as fast as MULVFS when used on MULVFS (and 20% faster than MULVFS when mounted on McLane Pumps) because of the low percent open area of the prefilter support plate. We think that the loss of particles is primarily due to the radial intake design (which channels water flow laterally through the filter holder) and its relatively short baffle length (which leads to increased turbulence at the prefilter), both of which enhance particle loss, especially when the particles are low in excess density. Living > 51 µm material (phytoplankton such as large diatoms and small non-motile zooplankton such as Acantharia) that is near neutrally buoyant is particularly prone to loss.

Liu et al. (2009) compared the efficiencies of four different filter holder designs at collecting particulate organic carbon (POC) and zooplankton. They used a 70 µm Teflon prefilter upstream of a 0.7 µm GF/F filter. Their "Pump 1" design was identical to our Holder C1 style, typically used for ^{234}Th applications. Their "Pump 2" was their Pump 1 design but with an additional 30 cm tall cylinder extending above the inlet. This is a design modification similar to that used by Bishop et al. (1986) to address evidence of particle loss evident during the first deployment of a four-filter version of the Large Volume

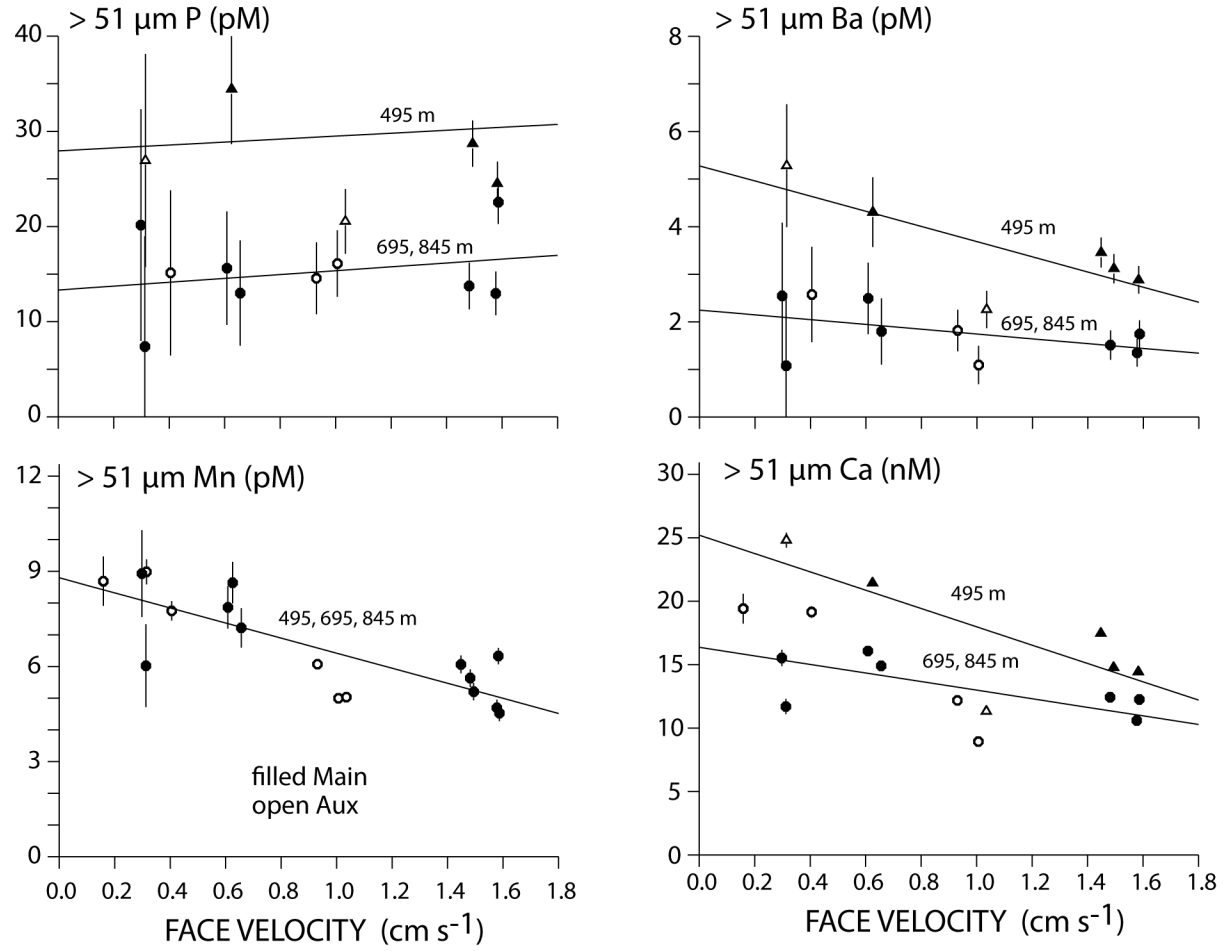

Fig. 17. > 51 µm P, Cd, Mn, and Ba concentrations at SAFe (MULVFS casts M7, M8, M9, M10) as a function of prefilter face velocity for main (filled symbols) and auxiliary (open symbols) filter holders for samples at 495 m (triangle symbols), 695 and 845 m (circle symbols). Only mini-MULVFS holder data are included here. Error bars are based on uncertainty of blank correction alone.

in-situ Filtration System (Bishop et al. 1980). Their "Pump 3" was a 293 mm filter holder with a sealed top and a central 5 cm wide elbow inlet, conceptually similar to our Holder D1 and manufactured by Challenger Oceanic. Finally, their "Pump 4" was a 293-mm filter holder manufactured by Challenger Oceanics, with a solid top and large radial intakes, conceptually similar to our holder B. The POC on their submicron GF/F filters (0.7-70 µm) varied by a factor of 3-4 between pumps, suggesting that each pump may have been sampling different particle populations, and consequently, complicating the comparison of the > 70 µm POC results. For the two pumps that had similar POC levels on the GF/F filters (Pumps 2 had 3.89 µM POC, and Pump 4 had 3.47 µM POC), the > 70 µm POC concentration from Pump 4 with the radial intake design was less than half that from Pump 2, with the extra 30 cm tall cylinder. While this is only a single comparison, it is nonetheless consistent with the hypothesis that the radial intake design enhances particle loss.

As noted in Liu et al. (2009), we found that an elbow intake style (Holders D1, D2, Liu's Pump 3) was more efficient at catching and retaining zooplankton, with the efficiency of zooplankton caught increasing with decreasing orifice size. This is likely because restricting the intake orifice for a given volume pump rate increases the velocity of the intake water so that zooplankton are unable to swim away. Because we are interested in suspended particulate matter rather than live zooplankton, the holders with large intake areas are preferable.

In summary, our filter holder intercomparisons suggest that many, if not all, previous designs of 142 mm filter holders experienced some loss of biogenic particles from the large size fraction. Until recently, the ^{234}Th community has been one of the biggest users of 142 mm filter holders. We obtained ^{234}Th activities from > 51 µm particles from a McLane holder (type B2) and a mini-MULVFS holder (type A2) from the pump-rosette experiment at SAFe. ^{234}Th activities were approximately 35% lower in the McLane rosette samples from 110 m compared with the mini-MULVFS holder (Maiti pers. comm.), and particulate phosphorus was also lower by a similar amount. This single comparison is encouraging, but we lack access to other McLane pump rosette and profile data from the IC

Table 4. Regression Statistics for Face Velocity (x, cm/s) vs. Elemental Concentration (pM for P, Ba, Mn; nM for Ca) at SAFe

Element	Depth (m)	Slope	Slope error	Intercept	Intercept error	y_error	r^2	*n*
P	345	4.180	26.39	54.069	29.920	15.932	0.019	7
	495	1.545	15.090	27.95	17.850	8.718	0.011	6
	695,845	2.027	5.028	13.33	5.086	4.228	0.064	10
Ba	495	–7.222	6.305	25.20	7.458	3.643	0.571	6
	345,495	–4.847	3.744	20.98	4.330	3.475	0.326	13
	695,845	–3.380	3.095	16.37	3.131	2.602	0.334	10
Ca	495	–1.593	1.350	5.28	1.597	0.780	0.586	6
	345,495	–1.434	0.904	5.40	1.046	0.839	0.421	13
	695,845	–0.504	0.644	2.25	0.651	0.541	0.205	10
Mn	495,695,845	–2.319	0.901	8.72	0.972	1.012	0.593	16
	incl. 345 m	–2.258	0.749	8.54	0.821	1.003	0.561	23

Errors are 95% confidence intervals.

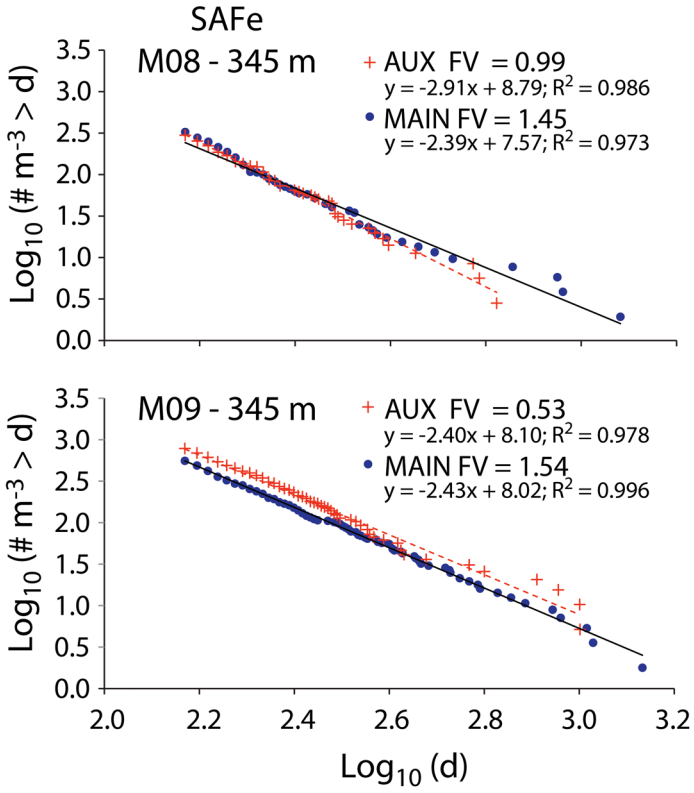

Fig. 18. Junge size-distributions for large particles (>150 µm) collected from 345 m during casts M8 and M9. Approximately 5% and 20% of main and auxiliary samples were analyzed. Data suggest little difference in aggregate distributions at face velocity (FV) of 0.99 and 1.45 cm s^{-1} (M08). The results for M09 suggest that aggregate populations are enhanced by 25% at FV = 0.53 cm s^{-1} versus FV 1.53 cm s^{-1}.

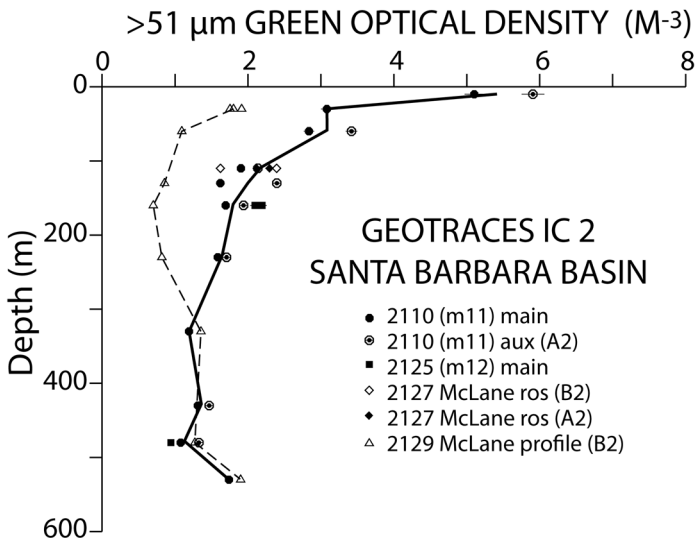

Fig. 19. Volume-scaled green optical density profiles for particles collected from the Santa Barbara Basin during MULVFS casts M11 and M12. Shown for comparison are data from McLane rosette casts 2127 and McLane pump profile 2129. Open symbol data use filter holder type B2, closed symbols use types A1 and A2.

experiments; we thus do not have enough data to draw any conclusion.

We have spent quite a lot of the discussion focusing on the large particle size fraction. At SAFe and BATS, it is certainly true that ~10% of the P was > 51 µm in size. On the other hand, well over 80% of the Sr and Ba were in the large particle size fraction in near surface waters. In biologically dynamic waters in all oceans, the > 51 µm fraction was often shown to contain more P, Si, and Ca than any other size fraction (e.g., Bishop and Edmond 1976; Bishop et al. 1978; Lam and Bishop 2007; Bishop and Wood 2008). Aggregate particles further permit micron-scale examination of processes key to understanding of the behavior of reactive chemical species such as Ba (Bishop 1988) and Fe (Lam and Bishop 2008). Thus sampling the large particle size fraction accurately is critically important to elemental budgets.

Moving forward into the GEOTRACES era, however, we have shown that Mn and Ba, which exist primarily as micron

and sub-micron–sized inorganic particulate phases, do behave differently than elements associated with biogenic material, and we expect that the suite of key trace elements and isotopes that will be measured on GEOTRACES will experience varying levels of fractionation with respect to biogenic material loss. It is thus crucial that a filter holder that does not experience particle loss is used for in-situ filtration. It is also a requirement for subsampling that particle distributions across filters be as uniform as possible.

Comments and recommendations

The GEOTRACES IC experiments in the Atlantic (2008) and Pacific (2009) permitted a comprehensive study of all aspects of in-situ filtration methodology by using the triple-flow path ability of MULVFS. This approach eliminated complications of different time, place, pump, and filter holder issues that have complicated past studies. Our recommendations permit in-situ filtration methodology to be robust and independent of the particular pumping system used or investigator.

For the smaller particle size fraction, we have demonstrated consistent profile results by in-situ filtration for a suite of particulate elements with contrasting behaviors to kilometer depths using samples collected using a variety of filter types, filter holder sizes (side arm to main), filter holder types, sample loadings, and flow rates. Element blanks for all filter types were controlled using in-situ blanks. In the case of phosphorus, we saw a 30% to 50% increased capture by 0.45 µm filters versus our standard set in near surface waters in oligotrophic regimes, consistent with the known dominance of these waters by picoplankton. Below the euphotic layer, the difference between the smaller pore size filters (in Side Arm samples) and the MULVFS standard set decreased to less than 10% (Fig. 5).

QMA filters are and remain far superior to Supor filters in terms of evenness of sample distribution and must be used for collection and analysis of the particulate organic fraction. QMA filters can also be used for determination of acid labile trace elements. The negative of QMA filters is that they only subsample down to a size limit of ~0.8 µm that they can adsorb elements like Al and U, which become problematic in low particle concentration waters, and that they can have a high blank level for many elements if they are subject to total digestion. We recommend the use of paired 0.8 µm Supor filters for collection of particles for analysis of trace metals where total digestion is required. The paired approach not only yields the equivalent sample collected by a 0.45 µm filter (Fig. 8), the second filter isolates the sub-micron fraction and thus yields insight into elemental partitioning amongst size classes. Paired 0.8 µm Supor filters allow far better particle loading (Fig. 6), better particle distribution (Fig. 7), and equivalent volume flow (Fig. 15) compared with a single 0.45 µm filter. In cases where an organic fraction is to be sampled, battery-powered pumps should be configured to collect samples in a twin flow path using separate holders loaded with QMA and Supor filters, as has been done for the US North Atlantic GEOTRACES section (GEOTRACES 2010). MULVFS pumps already permit parallel filtration using both QMA and Supor filters.

Loss of large particles is observed in all single- and double-baffled filter holder designs. We strongly recommend a filter holder design that has multiple baffle systems similar to MULVFS (A1) and mini-MULVFS (A2, Fig. 2). Details of these filter holders are included in this document and/or are published. Furthermore, pump systems must be configured with back flow preventing check valves and debubblers to minimize post filtration sample disturbance. Best samples are obtained when residual water in the filter holder is promptly removed by vacuum. This is simpler to do with 142 mm holders.

In-situ pumps appear to lose some particles due to partial fragmentation of large particles at average face velocities above 1 cm s^{-1} (through-mesh velocities above 3 cm s^{-1}). Losses appear to be independent of large particle size (Fig. 18) but different elements show different effects. We recommend modifications of pumps to operate below this limit. In the case of MULVFS, it is possible to moderate flow by emplacement of a flow-restricting orifice in the bottom stage of the main filter holder or by using paired 0.8 µm Supor filters in place of QMA filters. In the case of McLane pumps, it is possible to control flow rate via software, although this remains untested by our work.

As of this writing, McLane Research Laboratories has agreed to manufacture a commercial version of the mini-MULVFS filter holder and a dual-flow version of their standard pump, and expect such a product to be released in 2012.

Questions raised during review

One reviewer referred to a pump-pump intercomparison reported by Dunne et al. (1997) and suggested that MULVFS 1-53 µm POC data (Bishop 1999) were biased a factor of two lower compared with samples collected using a battery powered in situ pump system (Bacon et al. 1996). Two questions asked were: "Were less effective quartz filters used by Bishop et al. (1999) than those reported here?" and because one of us (Bishop) was fifth author on the Dunne et al. (1997) study, "Did this not mean that there was agreement on the Dunne et al. (1997) and assertion?" The answer to both questions is no. Bacon et al. (1996) and Bishop et al. (1999) document that identical Whatman QMA filters purposefully were used for sampling the 1-53 µm particle fraction (note: 53 µm mesh Nitex prefilters were used during JGOFS) to ensure intercomparability of results. Methodology for sample preservation was similar and POC analyses were performed using the same method and analyst. Blank correction was similar.

The first complication is that the profiles, although taken at the same geographic location near 0°N 140°W during the 1992 JGOFS Equatorial Pacific study, were collected 45 d apart. Factor of two differences in POC concentrations were indeed found in waters shallower than 100 m as reported by Dunne et al. (1997), yet the 1-53 µm POC values for the two profiles over the 100 m–500 m interval of common sampling agreed with one another within 5%. The waters sampled by Bacon et al. (1996) were different and more strongly stratified, as indi-

cated by potential density, temperature, and salinity profiles (http://usjgofs.whoi.edu/jg/dir/jgofs/eqpac/), and thus had conditions favorable to the modest factor-of-two higher levels of phytoplankton carbon biomass that Bacon et al. (1996) reported. Our findings that particle concentrations in the QMA fraction (1-51 µm) are consistent across a broad variety of filter holders lends further support that the differences reported by Dunne et al. (1997) are natural and not a sampling artifact. POC data from bottles, although offset high in profile compared to in-situ filtration, showed similar factor of two differences in surface waters for these same two expeditions. The factor of 2.2 scaling applied to MULVFS POC data by Dunne et al. (1997) was not justified by the data.

Also during review, the question of bottle versus pump particle concentration differences was also raised. Without going into exhaustive detail, efforts during the GEOTRACES intercomparison experiments show that bottles and pumps agree well for a diverse suite of particulate analytes when their filter blanks are properly assessed, contamination is avoided, consistent leaching or sample digestion methods are used, when samples are minimally handled, and when the sedimentation of particles in the bottles prior to sample filtration is considered (Planquette and Sherrell 2012; Bishop unpubl. data). This stands in contrast to particulate organic carbon (POC), where bottle data have been often reported to be much higher than those from in situ pumps (c.f. Altabet et al. 1992; Bishop et al. 1999; Gardner et al. 2003). The methodology for POC filtration often involves transfer of water from rosette bottle to one or more intermediate containers and gravity filtration in an open ship laboratory atmosphere using open filter funnels as was done during JGOFS cruises. The cases of best agreement between in-situ pump and bottle filtration have been when water is filtered directly in-line from the bottles (Altabet el al. 1992; Bishop et al. 2004, supplemental materials). We do recommend that a careful review of the methodology of bottle POC sampling and filtration to be undertaken.

References

Altabet, M. A., J. K. B. Bishop, and J. J. Mccarthy. 1992. Differences in particulate nitrogen concentration and isotopic composition for samples collected by bottles and large-volume pumps in gulf-stream warm-core rings and the Sargasso Sea. Deep-Sea Res. A 39: S405-S417 [doi:10.1016/S0198-0149(11)80022-1].

Bacon, M. P., and R. F. Anderson. 1982. Distribution of thorium isotopes between dissolved and particulate forms in the deep sea. J. Geophys. Res. 87:2045-2056 [doi:10.1029/JC087iC03p02045].

———, J. K. Cochran, D. Hirschberg, T. R. Hammar, and A. P. Fleer. 1996. Export flux of carbon at the equator during the EqPac time-series cruises estimated from ^{234}Th measurements. Deep-Sea Res. II 43:1133-1153 [doi:10.1016/0967-0645(96)00016-1].

Bishop, J. K. B. 1982. The effects of filtration speed on large particle catch during large volume in-situ filtration. EOS Trans. Amer. Geophys. Union 63:46.

———. 1988. The barite-opal-organic carbon association in oceanic particulate matter. Nature 332:341-343 [doi:10.1038/332341a0].

———. 1999. Transmissometer Measurement of POC. Deep-Sea Research I. 46(2) 353-369.

———, S. E. Calvert, and M. Y. S. Soon. 1999. Spatial and temporal variability of POC in the northeast Subarctic Pacific. Deep-Sea Res. II 46:2699-2733 [doi:10.1016/S0967-0645(99)00081-8].

———, and J. M. Edmond. 1976. New large volume filtration system for sampling of oceanic particulate matter. J. Mar. Res. 34:181-198.

———, R. W. Collier, D. R. Kettens, and J. M. Edmond. 1980. The Chemistry, Biology, and Vertical Flux of Particulate Matter from the Upper 1500m of the Panama Basin. Deep-Sea Research Part a-Oceanographic Research Papers 27: 615-640.

———, J. M. Edmond, D. R. Ketten, M. P. Bacon, and W. B. Silker. 1977. Chemistry, biology, and vertical flux of particulate matter from upper 400 M of equatorial Atlantic Ocean. Deep-Sea Res. 24:511-548 [doi:10.1016/0146-6291(77)90526-4].

———, and M. Q. Fleisher. 1987. Particulate manganese dynamics in Gulf-Stream Warm-Core Rings and surrounding waters of the NW Atlantic. Geochim. Cosmochim. Acta 51:2807-2825 [doi:10.1016/0016-7037(87)90160-8].

———, D. R. Ketten, and J. M. Edmond. 1978. Chemistry, Biology and Vertical Flux of Particulate Matter from the Upper 400m of the Cape Basin in the Southeast Atlantic Ocean. Deep-Sea Research 25: 1121-1161.

———, D. Schupack, R. M. Sherrell, and M. Conte. 1985. A multiple-unit large-volume in-situ filtration system for sampling oceanic particulate matter in mesoscale environments. Adv. Chem. Ser. 209:155-175 [doi:10.1021/ba-1985-0209.ch009].

———, J. C. Stepien, and P. H. Wiebe. 1986. Particulate matter distributions, chemistry and flux in the Panama Basin—Response to environmental forcing. Progr. Oceanogr. 17:1-59 [doi:10.1016/0079-6611(86)90024-8].

———, T. J. Wood, R. E. Davis, and J. T. Sherman. 2004. Robotic observations of enhanced carbon biomass and carbon export at 55S During SOFeX (Supplemental On-Line Materials). Science 304:417-420.

———, and T. J. Wood. 2008. Particulate matter chemistry and dynamics in the twilight zone at VERTIGO ALOHA and K2 sites. Deep Sea Res. I 55:1684-1706 [doi:10.1016/j.dsr.2008.07.012].

Buesseler, K. O., J. A. Andrews, M. C. Hartman, R. Belastock, and F. Chai. 1995. Regional estimates of the export flux of particulate organic carbon derived from thorium-234 during the JGOFS EqPac program. Deep Sea Research Part II: Topical Studies in Oceanography 42: 777-791.

———, and others. 2008. Particle fluxes associated with mesoscale eddies in the Sargasso Sea. Deep-Sea Res. II 55:1426-1444 [doi:10.1016/j.dsr2.2008.02.007].

Cutter, G. A., and K. W. Bruland. 2012. Rapid and noncontaminating sampling system for trace elements in global ocean surveys. Limnology and Oceanography: Methods 10: 425-436.

Dunne, J. P., J. W. Murray, J. Young, L. S. Balistrieri, and J. K. B. Bishop. 1997. ^{234}Th and particle cycling in the central equatorial pacific. Deep-Sea Res. II 44:2049-2083 [doi:10.1016/S0967-0645(97)00063-5].

Gardner, W. D., M. J. Richardson, C. A. Carlson, D. Hansell, and A. V. Mishonov. 2003. Determining true particulate organic carbon: bottles, pumps and methodologies. Deep Sea Res. II 50:655-674 [doi:10.1016/S0967-0645(02)00589-1].

GEOTRACES. 2006. GEOTRACES Science Plan. *In* S. C. o. O. Research [ed.]. <http://www.geotraces.org/libraries/documents/Science_plan.pdf>.

——— Standards and Intercalibration Committee [eds.]. 2010. Sampling and sample-handing protocols for GEOTRACES cruises. <http://www.obs-vlfr.fr/GEOTRACES/libraries/documents/Intercalibration/Cookbook.pdf>.

Krishnaswami, S., D. Lal, B. L. K. Somayajulu, R. F. Weiss, and H. Craig. 1976. Large volume in situ filtration of deep Pacific waters: mineralogical and radioisotope studies. Earth Planet. Sci. Lett. 32:420-429 [doi:10.1016/0012-821X(76)90082-0].

Lam, P. J., J. K. B. Bishop, C. C. Henning, M. A. Marcus, G. A. Waychunas, and I. Y. Fung. 2006. Wintertime phytoplankton bloom in the subarctic Pacific supported by continental margin iron. Global Biogeochem. Cycl. 20 [doi:10.1029/2005GB002557].

———, and J. K. B. Bishop. 2007. High biomass low export regimes in the Southern Ocean. Deep Sea Res. II 54:601-638 [doi:10.1016/j.dsr2.2007.01.013].

———, and ———. 2008. The continental margin is a key source of iron to the HNLC North Pacific Ocean. Geophys. Res. Lett. 35:L07608.

Liu, Z., and others. 2005. Why do POC concentrations measured using Niskin bottle collections sometimes differ from those using in-situ pumps? Deep Sea Res. I 52:1324-1344 [doi:10.1016/j.dsr.2005.02.005].

———, J. K. Cochran, C. Lee, B. Gasser, J. C. Miquel, and S. G. Wakeham. 2009. Further investigations on why POC concentrations differ in samples collected by Niskin bottle and in situ pump. Deep Sea Res. II 56:1558-1567 [doi:10.1016/j.dsr2.2008.12.019].

Maiti, K., et al. In press. Intercalibration studies of short-lived thorium-234 in the water column and marine particles. Limnol. Oceanogr. Methods.

Morrison, A. T., III, J. D. Billings, and K. W. Doherty. 2000. The McLane WTS-LV: A Large Volume, High Accuracy Oceanographic Sampling Pump, p. 847-852. Oceans 2000 MTS/IEEE Conference and Exhibition.

Planquette, H., and R. M. Sherrell. 2012. Intercal: Sampling for particulate trace metal determinaton using water sampling bottles: comparison to in situ pumps. Limnol. Oceanogr. Methods 10:367-388.

Sachs, P. L., T. R. Hammar, and M. P. Bacon. 1989. A large-volume, deep-sea submersible pumping system. Woods Hole Oceanographic Institution Technical Report. WHOI. < https://darchive.mblwhoilibrary.org/bitstream/handle/1912/4611/WHOI-89-55.pdf?sequence=1>.

Sherrell, R. M. 1991. Collection of suspended particulate matter for trace metal analysis using a new in-situ pump, p. 285-294. *In* D. C. Hurd and D. W. Spencer [eds.], Marine particles: analysis and characterization. American Geophysical Union.

———, and E. A. Boyle. 1992. Isotopic Equilibration between Dissolved and Suspended Particulate Lead in the Atlantic-Ocean - Evidence from Pb-210 and Stable Pb Isotopes. Journal of Geophysical Research-Oceans 97: 11257-11268.

Siegel, D. A., T. D. Dickey, L. Washburn, M. K. Hamilton, and B. G. Mitchell. 1989. Optical determination of particulate abundance and production variations in the oligotrophic ocean. Deep Sea Research Part A. Oceanographic Research Papers 36: 211-222.

Simpson, W. R., T. J. P. Gwilliam, V. A. Lawford, R. A. Lewis, and M. J. R. Fasham. 1987. An in situ deep water particle sampler and real-time sensor package with data from the Madeira Abyssal Plain. Deep-Sea Res. 34:1477-1497 [doi:10.1016/0198-0149(87)90138-5].

Wakeham, S. G., and E. A. Canuel. 1988. Organic geochemistry of particulate matter in the eastern tropical North Pacific Ocean: implications for particle dynamics. J. Mar. Res. 46:183-213 [doi:10.1357/002224088785113748].

Submitted 30 October 2011
Revised 19 March 2012
Accepted 19 April 2012